Flussi dissipativi in una dimensione

$$\frac{1}{L}\frac{dL}{dt} = \frac{1}{L}\left[f(X_B) - f(X_A)\right] = \frac{df(X)}{dX} < 0$$

fixed points (dim.0)

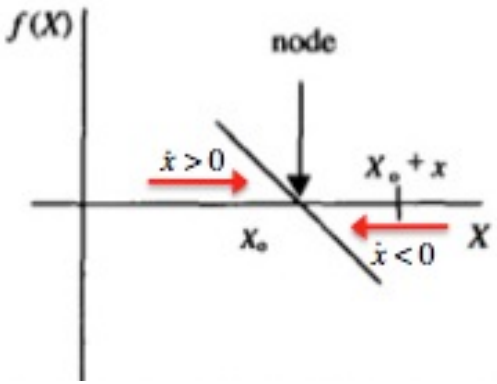

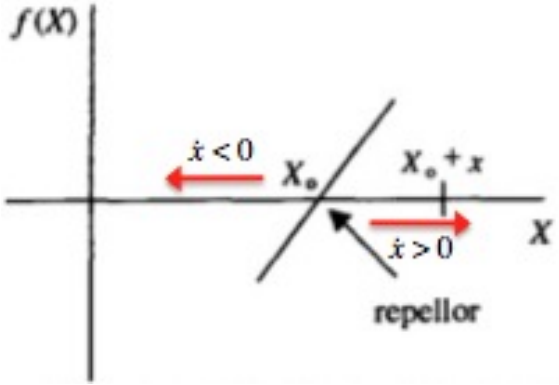

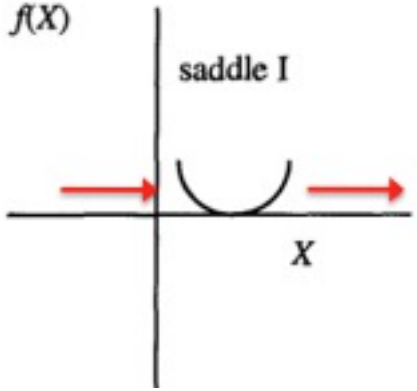

Flussi dissipativi in due dimensioni

$$\frac{1}{A}\frac{dA}{dt} = \frac{\partial f_1}{\partial X_1} + \frac{\partial f_2}{\partial X_2} < 0$$

fixed points (dim.0)

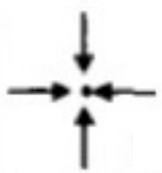

NODE

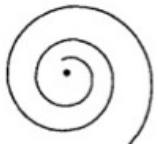

SPIRAL NODE

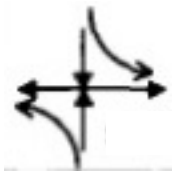

SADDLE POINTS

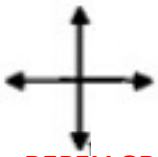

REPELLOR

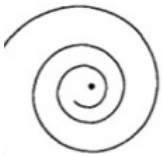

SPIRAL REPELLOR

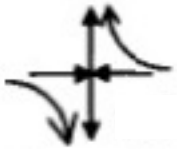

limit cycles (dim.1)

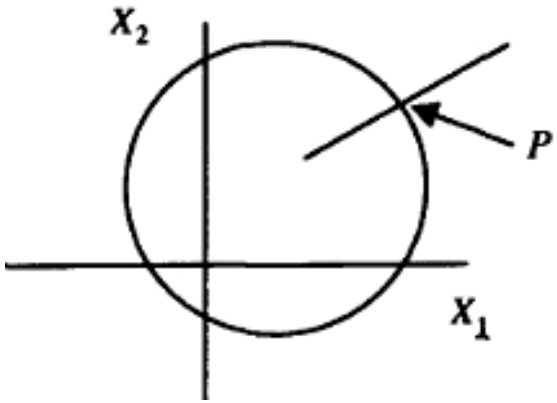

Flussi dissipativi in tre dimensioni

Cluster di condizioni iniziali

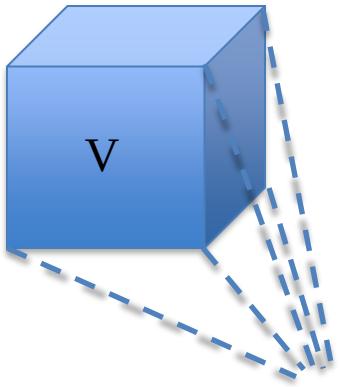

$$\frac{1}{V}\frac{dV}{dt} = \sum_{i=1}^{N} \frac{\partial f_i}{\partial x_i} \equiv div(f) \quad < 0$$

$$\begin{cases} \dot{x}_1 = f_1(x_1, x_2, x_3) \\ \dot{x}_2 = f_2(x_1, x_2, x_3) \\ \dot{x}_3 = f_3(x_1, x_2, x_3) \end{cases}$$

ATTRATTORI

- fixed points (dim.0)
- limit cycles (dim.1)
- quasiperiodic attractors (dim.2)
- chaotic attractors (fractal dimension between 2 and 3)

Flussi dissipativi in tre dimensioni

Cluster di condizioni iniziali

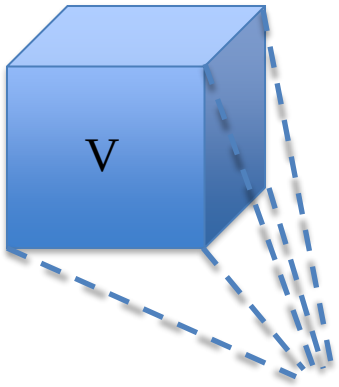

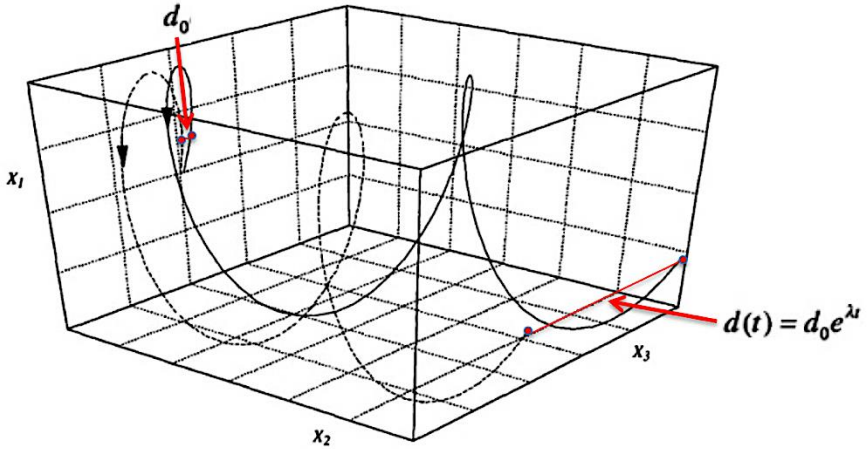

ATTRATTORI

1. no intersection of different trajectories;
2. bounded trajectories;
3. exponential divergence of nearby trajectories.

chaotic attractors (fractal dimension between 2 and 3)

Flussi dissipativi in tre dimensioni

Cluster di condizioni iniziali

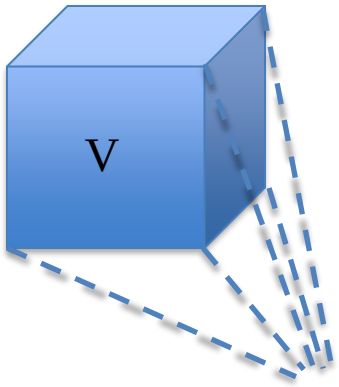

$$\frac{1}{V}\frac{dV}{dt} = \sum_{i=1}^{N} \frac{\partial f_i}{\partial x_i} \equiv div(f) \quad < 0$$

ATTRATTORI

fixed points (dim.0)

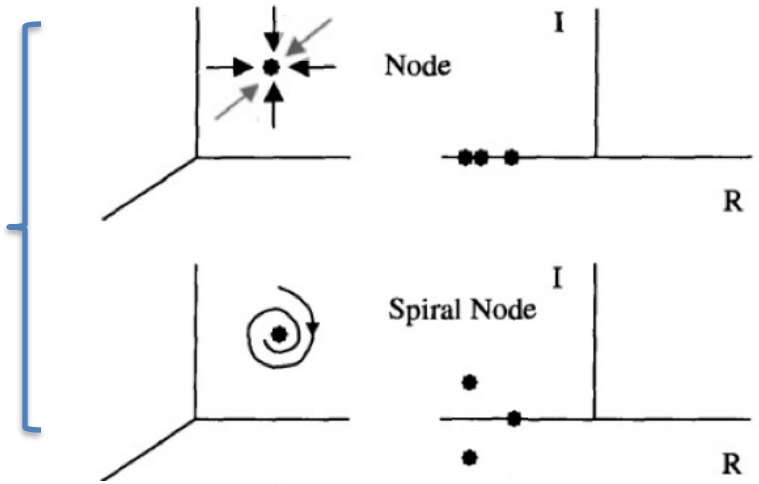

$$J = \begin{pmatrix} \frac{\partial f_1}{\partial x_1} & \frac{\partial f_1}{\partial x_2} & \frac{\partial f_1}{\partial x_3} \\ \frac{\partial f_2}{\partial x_1} & \frac{\partial f_2}{\partial x_2} & \frac{\partial f_2}{\partial x_3} \\ \frac{\partial f_3}{\partial x_1} & \frac{\partial f_3}{\partial x_2} & \frac{\partial f_3}{\partial x_3} \end{pmatrix}$$

Flussi dissipativi in tre dimensioni

Cluster di condizioni iniziali

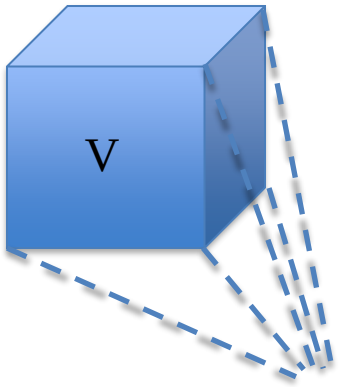

$$\frac{1}{V}\frac{dV}{dt} = \sum_{i=1}^{N} \frac{\partial f_i}{\partial x_i} \equiv div(f) \quad < 0$$

ATTRATTORI

fixed points (dim.0)

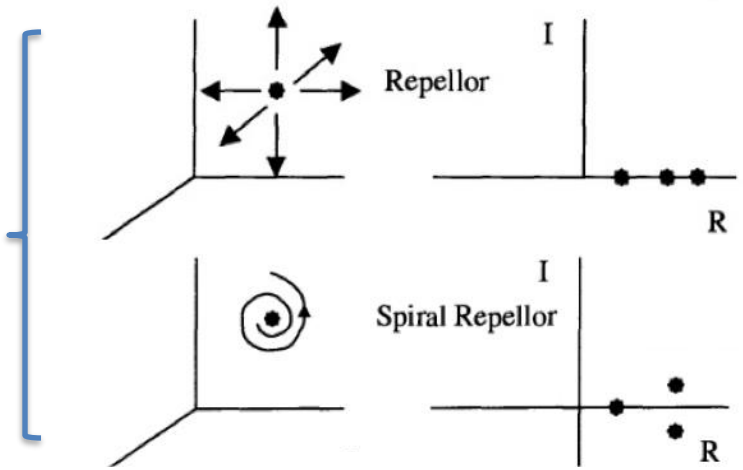

$$J = \begin{pmatrix} \frac{\partial f_1}{\partial x_1} & \frac{\partial f_1}{\partial x_2} & \frac{\partial f_1}{\partial x_3} \\ \frac{\partial f_2}{\partial x_1} & \frac{\partial f_2}{\partial x_2} & \frac{\partial f_2}{\partial x_3} \\ \frac{\partial f_3}{\partial x_1} & \frac{\partial f_3}{\partial x_2} & \frac{\partial f_3}{\partial x_3} \end{pmatrix}$$

Flussi dissipativi in tre dimensioni

Cluster di condizioni iniziali

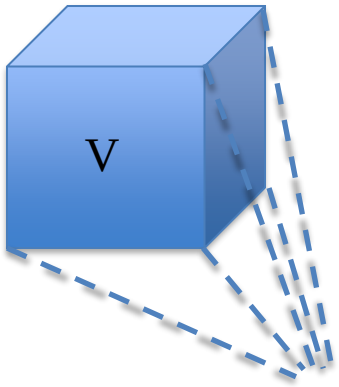

$$\frac{1}{V}\frac{dV}{dt} = \sum_{i=1}^{N} \frac{\partial f_i}{\partial x_i} \equiv div(f) \quad < 0$$

ATTRATTORI

fixed points (dim.0)

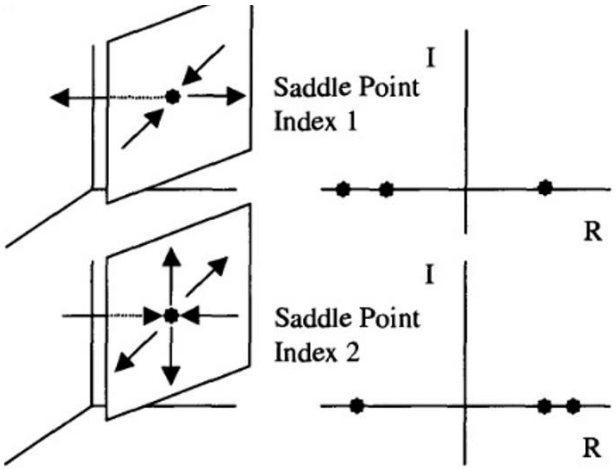

$$J = \begin{pmatrix} \frac{\partial f_1}{\partial x_1} & \frac{\partial f_1}{\partial x_2} & \frac{\partial f_1}{\partial x_3} \\ \frac{\partial f_2}{\partial x_1} & \frac{\partial f_2}{\partial x_2} & \frac{\partial f_2}{\partial x_3} \\ \frac{\partial f_3}{\partial x_1} & \frac{\partial f_3}{\partial x_2} & \frac{\partial f_3}{\partial x_3} \end{pmatrix}$$

Flussi dissipativi in tre dimensioni

Cluster di condizioni iniziali

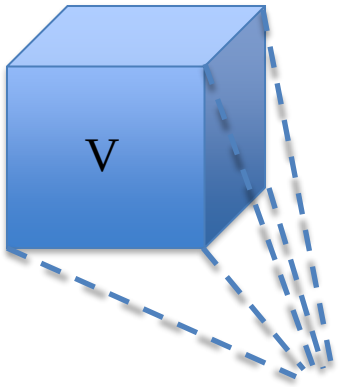

$$\frac{1}{V}\frac{dV}{dt} = \sum_{i=1}^{N} \frac{\partial f_i}{\partial x_i} \equiv div(f) \quad < 0$$

ATTRATTORI

fixed points (dim.0)

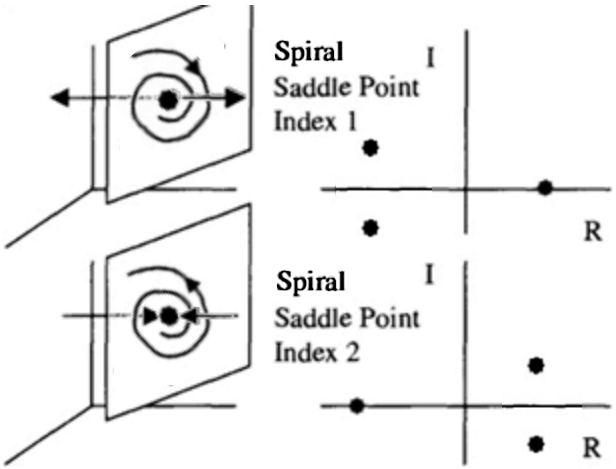

$$J = \begin{pmatrix} \frac{\partial f_1}{\partial x_1} & \frac{\partial f_1}{\partial x_2} & \frac{\partial f_1}{\partial x_3} \\ \frac{\partial f_2}{\partial x_1} & \frac{\partial f_2}{\partial x_2} & \frac{\partial f_2}{\partial x_3} \\ \frac{\partial f_3}{\partial x_1} & \frac{\partial f_3}{\partial x_2} & \frac{\partial f_3}{\partial x_3} \end{pmatrix}$$

4.6 Limit Cycles and Poincaré Sections (dim = 1)

As we saw in Chapter 3, dynamical systems in two (and higher) dimensions can also settle into long-term behavior associated with repetitive, periodic limit cycles. We also learned that the Poincaré section technique can be used to reduce the dimensionality of the description of these limit cycles and to make their analysis simpler.

First, we focus on the construction of a Poincaré section for the system. For a three-dimensional state space, the Poincaré section is generated by choosing a ***Poincaré plane*** (a two-dimensional surface) and recording on that surface the points at which a given trajectory cuts through that surface. (In most cases the choice of plane is not crucial as long as the trajectories cut the surface ***transversely***, that is, the trajectories do not run parallel or almost parallel to the surface as they pass through; see Fig. 4.4.) For autonomous systems, such as the Lorenz model equations, we choose some convenient plane in the state space, say, the XY plane for the Lorenz equations. When a trajectory crosses that plane passing from, for example, negative Z values to positive Z values, we record that crossing point.

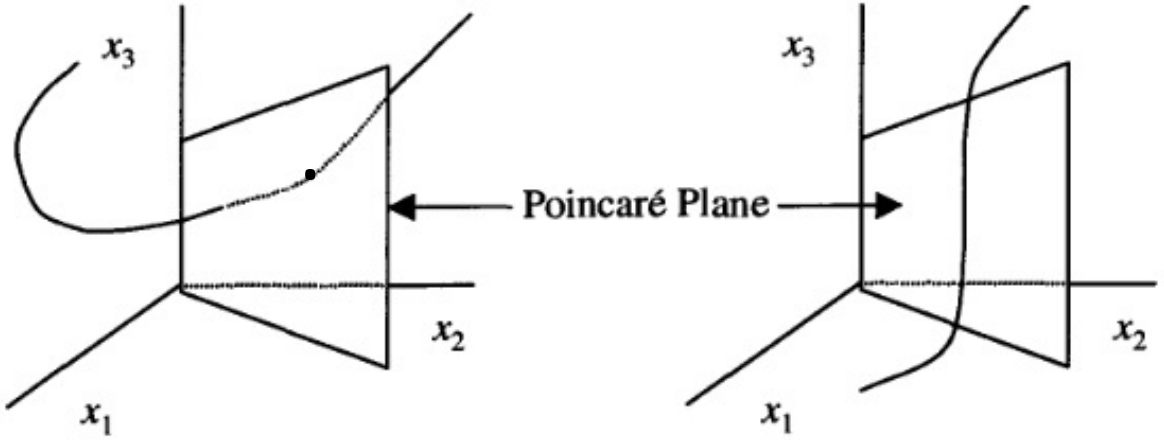

Fig. 4.4. A Poincaré section for a three-dimensional state space. On the left the trajectory crosses the Poincaré plane transversely. On the right the intersection is not transverse because the trajectory runs parallel to the plane for some distance.

In later discussions, it will be useful to indicate on the Poincaré section the record of trajectory intersections with the plane as trajectories approach or diverge from the periodic points. For example, Fig. 4.6 shows a sequence of points $P_0, P_1, P_2, \ldots$ as a trajectory approaches an attracting limit cycle in a three-dimensional state space. (Compare Fig. 4.6 with Fig. 3.13.) The reader should be warned that in some diagrams found in the literature this series of dots will be connected with a smooth curve intersecting (x_1^*, x_2^*). It is important to remember that this curve is not a trajectory. In fact the Poincaré intersection of any single trajectory is just a sequence of points as shown in Fig. 4.6. If a smooth curve is drawn on this kind of diagram, it represents the intersection points of an infinite family of trajectories, all of which are approaching (x_1^*, x_2^*). Later we shall see cases in which such curves intersect. It is important to remember that this intersection does not violate the No-Intersection Theorem because the intersecting curves in this case are not themselves trajectories.

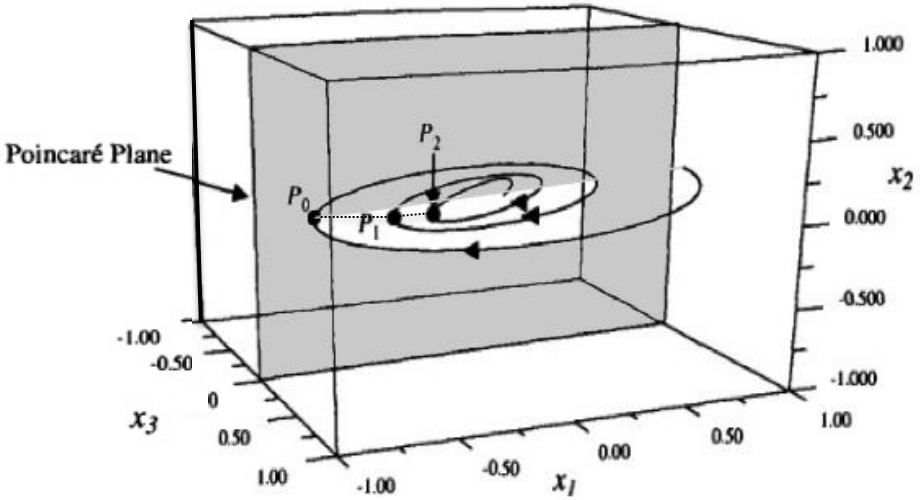

Fig. 4.6. The sequence of points $P_0, P_1, P_2, \ldots$ is the record of successive intersections of a single trajectory with the Poincaré plane (the plane with $x_3 = 0$) as the trajectory goes from $x_3 > 0$ to $x_3 < 0$.

MAPPA DI POINCARE' 2D PER LO STUDIO DELLA STABILITA' DEI CICLI LIMITE IN 3D

We now return to the general discussion of limit cycles. The stability of the limit cycle is determined by a generalization of the Poincaré multipliers introduced in the previous chapter. We assume that the uniqueness of the solutions to the equations used to describe the dynamical system entails the existence of a Poincaré map function (or in the present case, a pair of Poincaré map functions), which relate the coordinates of one point at which the trajectory crosses the Poincaré plane to the coordinates of the next (in time) crossing point. (Again we assume we have chosen a definite crossing sense; e.g., from top to bottom, or from left to right.) These functions take the form

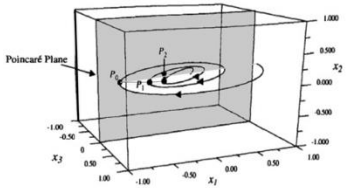

$$x_1^{(n+1)} = F_1(x_1^{(n)}, x_2^{(n)})$$
$$x_2^{(n+1)} = F_2(x_1^{(n)}, x_2^{(n)}) \qquad (4.6\text{-}1)$$

mappa di Poincarè 2 dim

where the parenthetical superscript indicates the crossing point number.

Here these Poincaré map functions have arisen from the consideration of a Poincaré section for trajectories arising from a set of differential equations. In Chapter 5, we shall consider such map functions as interesting models in their own right, independent of this particular heritage.

The fixed points of the Poincaré section are those points that satisfy

$$x_1^* = F_1(x_1^*, x_2^*)$$
$$x_2^* = F_2(x_1^*, x_2^*) \qquad (4.6\text{-}2)$$

Each fixed point in the Poincaré section corresponds to a limit cycle in the full three-dimensional state space.

MAPPA DI POINCARE' 2D PER LO STUDIO DELLA STABILITA' DEI CICLI LIMITE IN 3D

We can characterize the stability of these fixed points by finding the characteristic values of the associated Jacobian matrix of derivatives [sometimes called the ***Floquet matrix***, after Gaston Floquet (1847–1920), a French mathematician who studied, among other things, the properties of differential equations with periodic terms]. This matrix is analogous to the Jacobian matrix used to determine the characteristic values of a fixed point in the full state space. The Jacobian matrix *JM* is given by

mappa 1 dim

$$d_2 = Md_1$$

$$d_{n+1} = M^n d_1$$

$$M = \left.\frac{dF}{dP}\right|_{P^*}$$

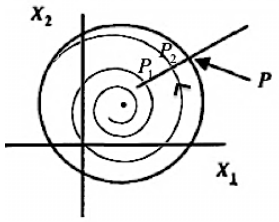

mappa 2 dim

$$JM = \begin{pmatrix} \frac{\partial F_1}{\partial x_1} & \frac{\partial F_1}{\partial x_2} \\ \frac{\partial F_2}{\partial x_1} & \frac{\partial F_2}{\partial x_2} \end{pmatrix} \longrightarrow \begin{matrix} M_1 \\ M_2 \end{matrix} \qquad (4.6\text{-}3)$$

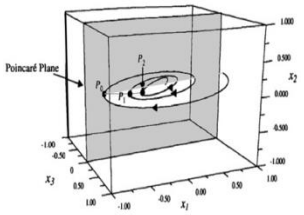

where the matrix is to be evaluated at the Poincaré map fixed point in question. The characteristic values of this matrix determine the stability of the limit cycle. A stable limit cycle attracts nearby trajectories, while an unstable limit cycle repels nearby trajectories. In principle, we can use the mathematical methods given in Chapter 3 to find these characteristic values. In practice, however, we most often cannot find these characteristic values explicitly, since, to do that, we would need to know the exact form of the Poincaré map function, and in most cases, we do not know that function. [In Chapter 5, we will examine some models that do give us the map function directly. However, for systems described by differential equations in state spaces of three (or more) dimensions, it is in general impossible to find the map functions.]

Stability of Limit Cycles

As we saw in two-dimensional systems, if the fixed point is to be stable and have trajectories in its neighborhood attracted to it, then the *absolute value* of each multiplier must be less than 1. [In state spaces with three or more dimensions, we can have $M < 0$; so the stability criterion is formulated using the absolute value of the multipliers.]

The types of limit cycles are

I. ***Stable limit cycle*** (node for the Poincaré map)
II. ***Repelling limit cycle*** (repellor for the Poincaré map)
III. ***Saddle cycle*** (saddle point for the Poincaré map)

Table 4.2 lists the categories of characteristic multipliers, the associated Poincaré plane fixed points and the corresponding limit cycles for three-dimensional state spaces. (Compare this table to Table 3.4 for limit cycles in two-dimensional state spaces.)

Table 4.2
Characteristic Multipliers for Poincaré Sections of Three-Dimensional State Spaces

Type of Fixed Point	Characteristic Multiplier	Corresponding Cycle
Node	$\lvert M_1\rvert, \lvert M_2\rvert < 1$	Limit Cycle
Repellor	$\lvert M_1\rvert, \lvert M_2\rvert > 1$	Repelling Cycle
Saddle	$\lvert M_1\rvert < 1, \lvert M_2\rvert > 1$	Saddle Cycle

Of course, the characteristic multipliers could also be complex numbers. Just as we saw for fixed points in a two-dimensional state space, the complex multipliers will form a complex-conjugate pair. In more graphic terms, the successive Poincaré intersection points associated with complex-valued multipliers rotate around the limit cycle intersection point as they approach or diverge from that point. Mathematically, the condition for stability is still the same: the absolute value of both multipliers must be less than 1 for a stable limit cycle. In terms of the corresponding Argand diagram (complex mathematical plane), both characteristic values must lie within a circle of unit radius (called the ***unit circle***) for a stable limit cycle. See Fig. 4.7. As a control parameter is changed the values of the characteristic multipliers can change. If at least one of the characteristic multipliers crosses the unit circle, a bifurcation occurs. Some of these bifurcations will be discussed in the latter part of this chapter.

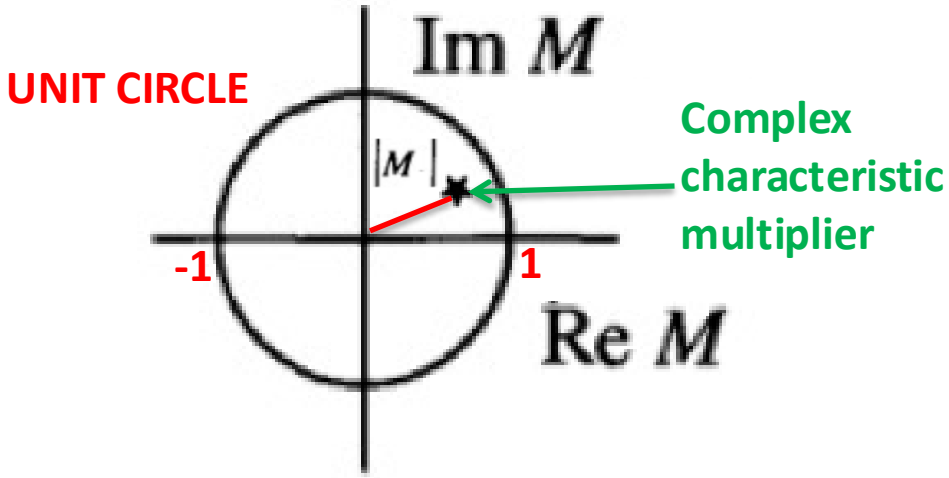

Stable Limit Cycles

$|M_1|, |M_2| < 1$

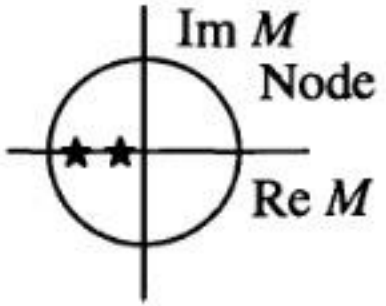

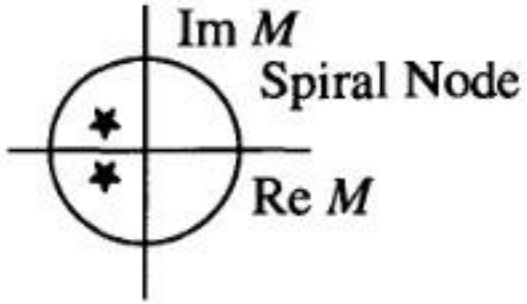

Repelling Limit Cycles

$|M_1|, |M_2| > 1$

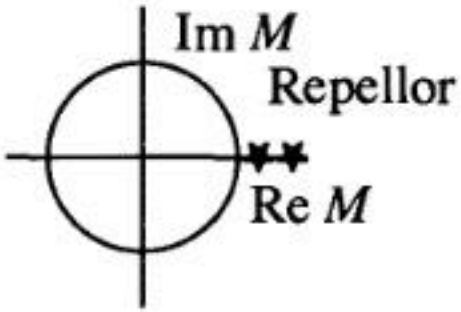

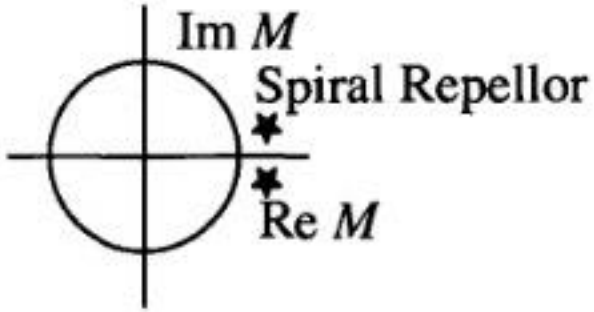

Saddle Limit Cycles

$|M_1| < 1, |M_2| > 1$

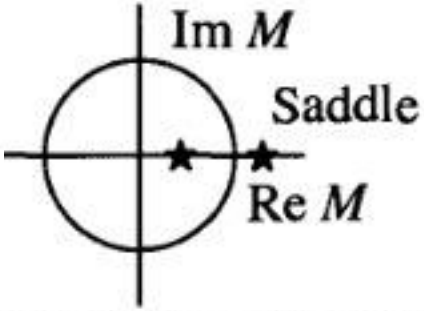

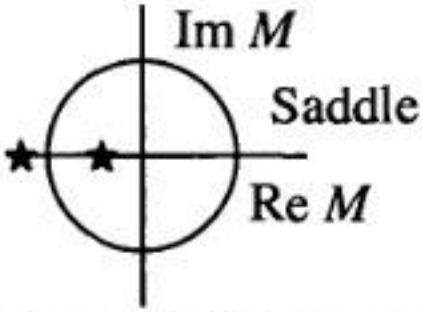

Fig. 4.7. Characteristic multipliers in the complex plane. If both multipliers lie within a circle of unit radius (the unit circle), then the corresponding limit cycle is stable. If one (or both) of the multipliers lies outside the unit circle, then the limit cycle is unstable.

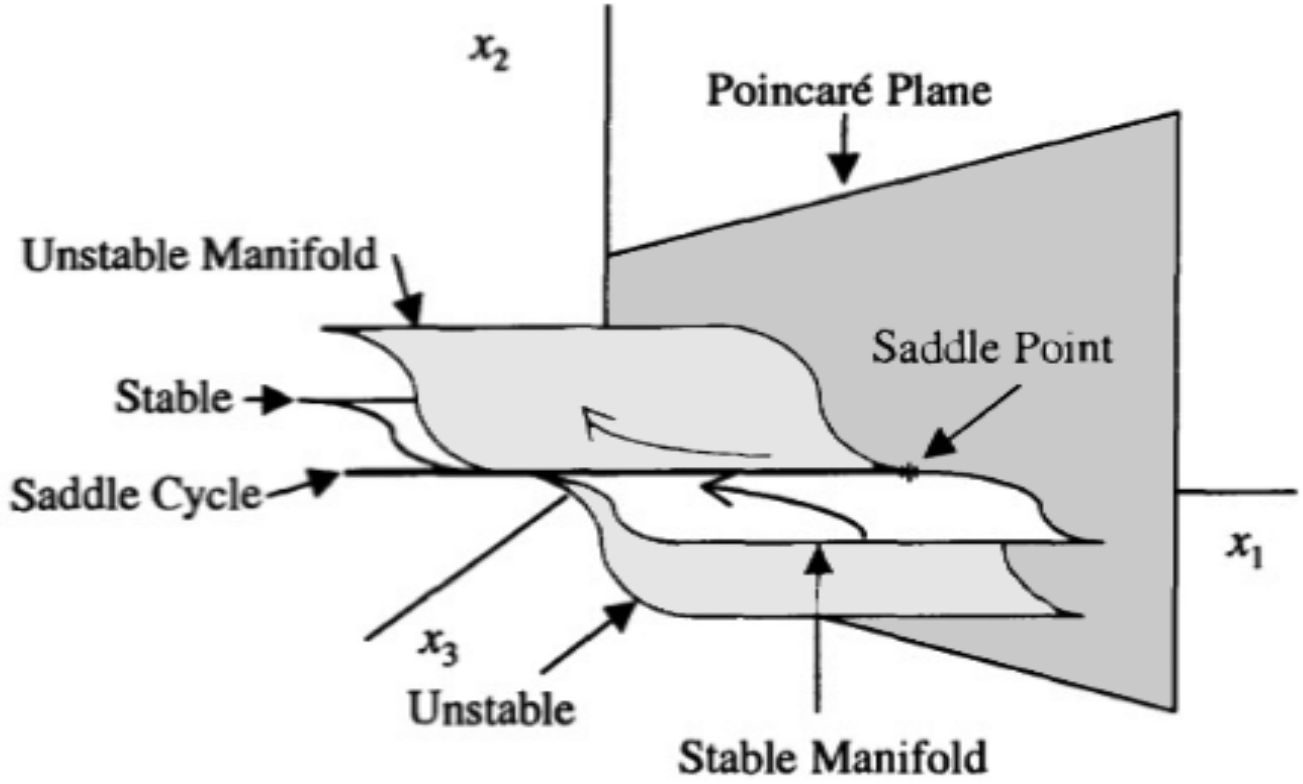

Saddle

Limit Cycles

$|M_1| < 1, |M_2| > 1$

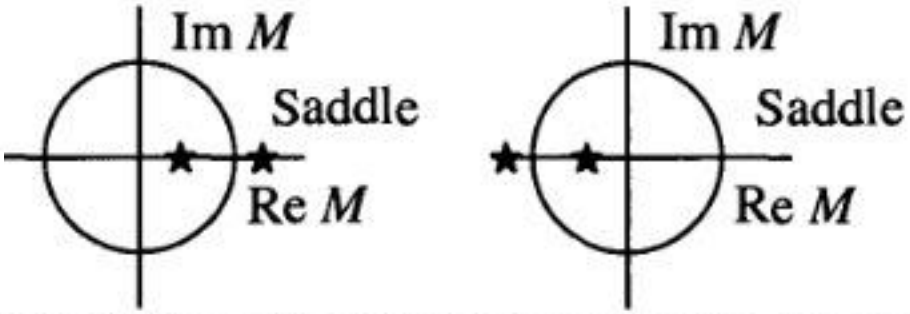

Fig. 4.7. Characteristic multipliers in the complex plane. If both multipliers lie within a circle of unit radius (the unit circle), then the corresponding limit cycle is stable. If one (or both) of the multipliers lies outside the unit circle, then the limit cycle is unstable.

4.7 Quasi-Periodic Behavior (dim = 2)

For a three-dimensional state space, a new type of motion can occur, a type of motion not possible in one- or two-dimensional state spaces. This new type of motion is called *quasi-periodic* because it has two different frequencies associated with it; that is, it can be analyzed into two independent, periodic motions. For quasi-periodic motion, the trajectories are constrained to the surface of a torus in the three-dimensional state space. A mathematical description of this kind of motion is given by:

NOTA BENE: NON SONO EQUAZIONI DIFFERENZIALI!

Equazioni della traiettoria di un punto (x_1(t), x_2(t) *e* x_3(t)) sull'attrattore quasiperiodico

$$\begin{aligned} x_1 &= (R + r\sin\omega_r t)\cos\omega_R t \\ x_2 &= r\cos\omega_r t \\ x_3 &= (R + r\sin\omega_r t)\sin\omega_R t \end{aligned} \qquad (4.7\text{-}1)$$

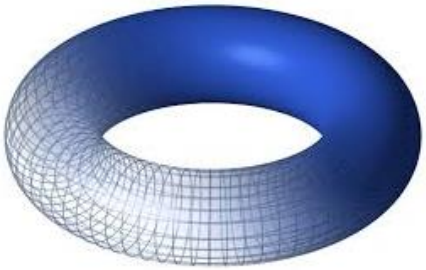

where the two angular frequencies are denoted by ω_R and ω_r. Geometrically, Eqs. (4.7-1) describe motion on the surface of a torus (with the center of the torus at the origin), whose large radius is R and whose cross-sectional radius is r. In general the torus (or doughnut-shape or the shape of the inner tube of a bicycle tire) will look something like Fig. 4.8. The frequency ω_R corresponds to the rate of rotation around the large circumference with a period $T_R = 2\pi/\omega_R$, while the frequency ω_r corresponds to the rate of rotation about the cross section with $T_r = 2\pi/\omega_r$. A general torus might have elliptical cross sections, but the ellipses can be made into circles by suitably rescaling the coordinate axes.

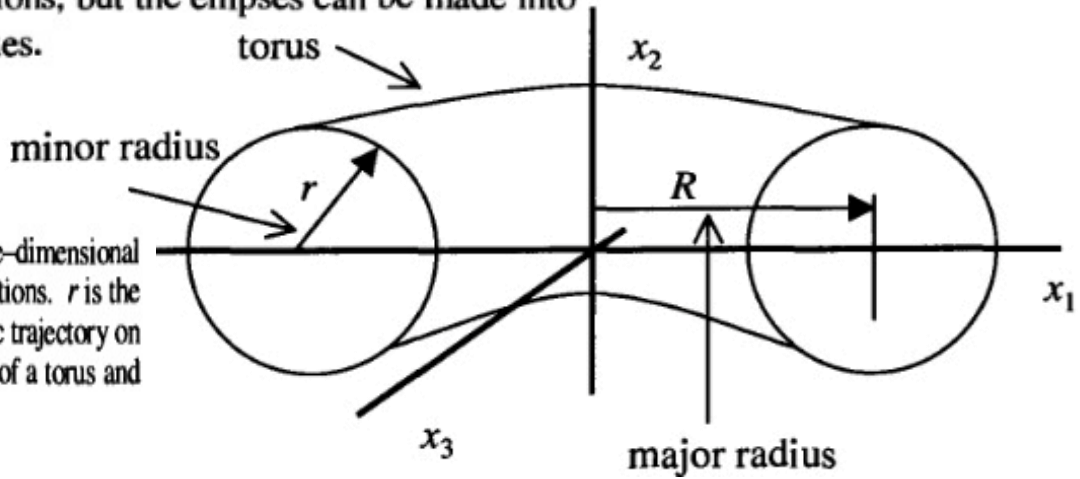

Fig. 4.8. Quasi-periodic trajectories roam over the surface of a torus in three-dimensional state space. Illustrated here is the special case of a torus with circular cross sections. r is the minor radius of the cross section. R is the major radius of the torus. A periodic trajectory on the surface of the torus would close on itself. On the right, a perspective view of a torus and a Poincaré plane.

The Poincaré section for this motion is generated by using a Poincaré plane that cuts through the torus. What the pattern of Poincaré map points looks like depends on the numerical relationship between the two frequencies as illustrated in Fig. 4.9. If the ratio of the two frequencies can be expressed as the ratio of two integers (that is, as a "rational fraction," 14/17, for example), then the Poincaré section will consist of a finite number of points. This type of motion is often called ***frequency-locked*** motion because one of the frequencies is locked, often over a finite control parameter range, so that an integer multiple of one frequency is equal to another integer multiple of the other. (The terms ***phase-locking*** and ***mode-locking*** are also used to describe this behavior.)

$\frac{w_R}{w_r}$

Winding Number razionale

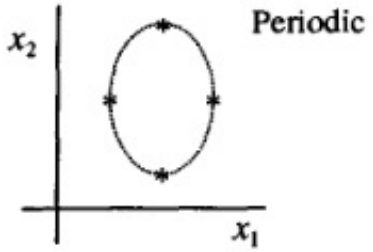

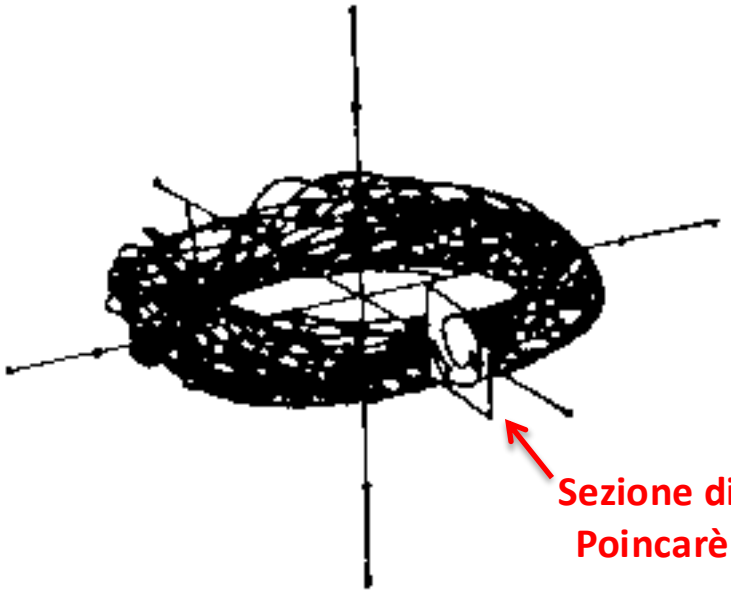

Fig. 4.9. A Poincaré section intersects a torus in three–dimensional state space. The diagram on the upper left shows the Poincaré map points for a two-frequency periodic system with a rational ratio of frequencies. The intersection points are indicated by asterisks. The diagram on the lower left is for quasi-periodic behavior. The ratio of frequencies is irrational, and eventually the intersection points fill in a curve (sometimes called a "drift ring") in the Poincaré plane.

If the ratio of frequencies cannot be expressed as a ratio of integers, then the ratio is called "irrational" (in the mathematical, not the psychological sense). For the irrational case, the Poincaré map points will eventually fill in a continuous curve in the Poincaré plane, and the motion is said to be ***quasi-periodic*** because the motion never exactly repeats itself. (Russian mathematicians call this ***conditionally periodic***. See, for example, [Arnold, 1983]. The term ***almost periodic*** is also used in the mathematical literature.)

In the quasi-periodic case the motion, strictly speaking, never exactly repeats itself (hence, the modifier *quasi*), but the motion is not chaotic; it is composed of two (or more) periodic components, whose presence could be made known by measuring the frequency spectrum (Fourier power spectrum) of the motion. We should point out that detecting the difference between quasi-periodic motion and motion with a rational ratio of frequencies, when the integers are large, is a delicate question. Whether a given experiment can distinguish the two cases depends on the resolution of the experimental equipment. As we shall see later, the behavior of the system can switch abruptly back and forth between the two cases as a parameter of the system is varied. The important point is that the attractor for the system is a two-dimensional surface of the torus for quasi-periodic behavior.

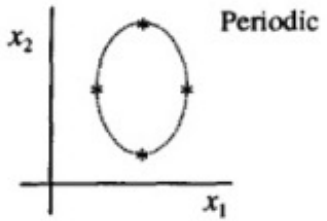

Winding Number irrazionale

$$\frac{w_R}{w_r}$$

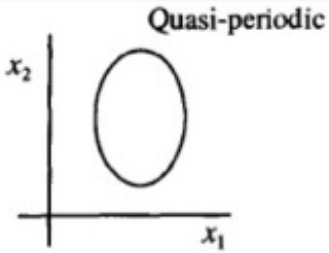

Sezione di Poincarè

quasi-periodicity.nlogo

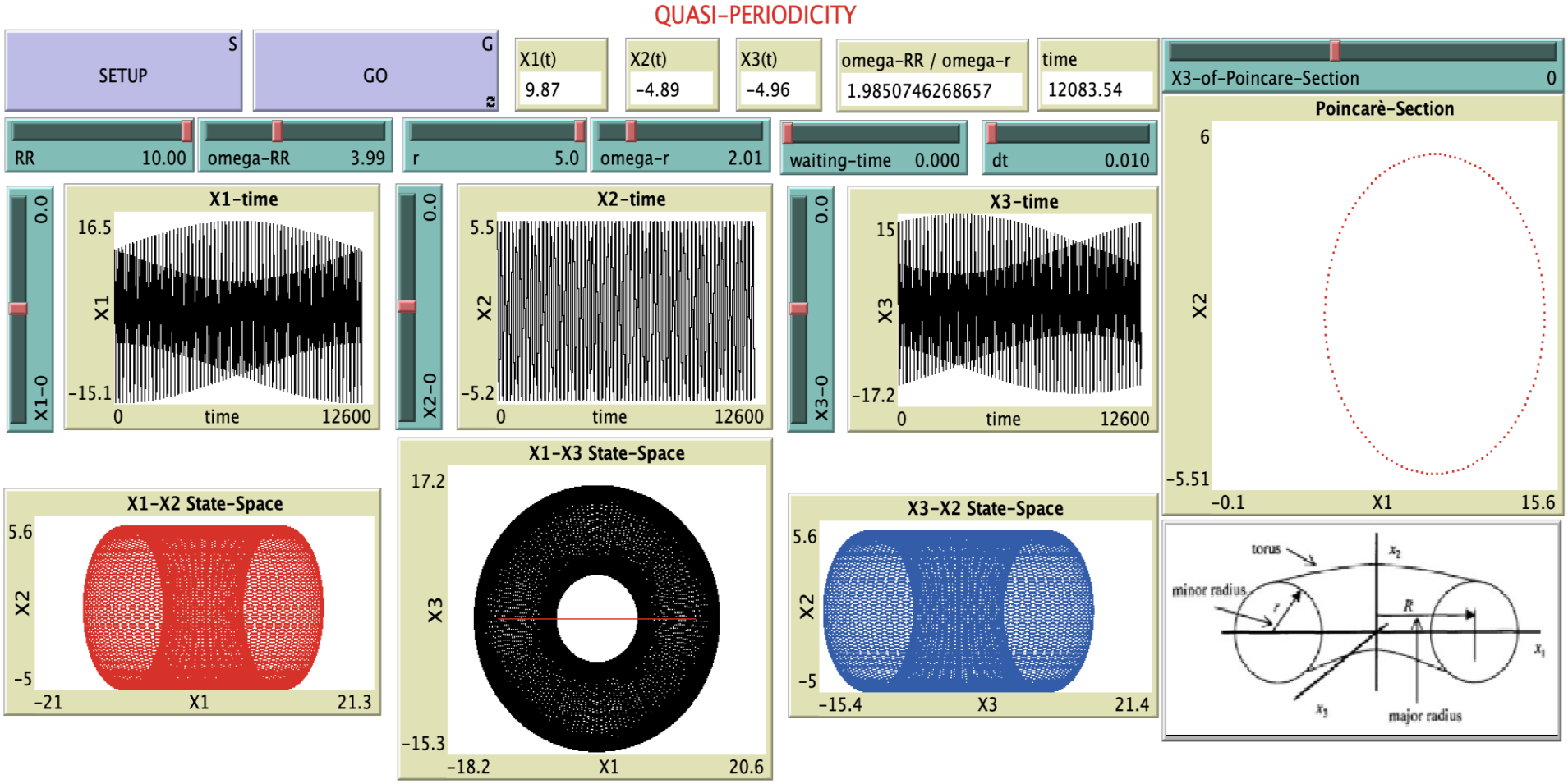

We have now seen the full panoply of regular (nonchaotic) attractors: fixed points (dimension 0), limit cycles (dimension 1), and quasi-periodic attractors (dimension 2 or more). We are ready to begin the discussion of how these attractors can change into chaotic attractors.

We will give only a brief discussion of the period-doubling, quasi-periodic, and intermittency routes. These will be discussed in detail in Chapters 5, 6, and 7, respectively. A discussion of crises will be found in Chapter 7. As we shall see, the chaotic transient route is more complicated to describe because it requires a knowledge of what trajectories are doing over a range of state space. We can no longer focus our attention locally on just a single fixed point or limit cycle.

fixed points (dim.0)

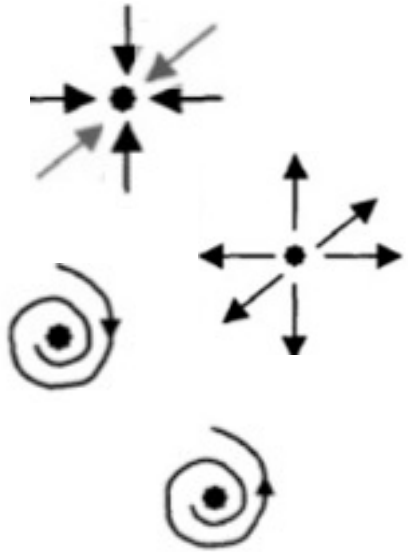

limit cycles (dim.1)

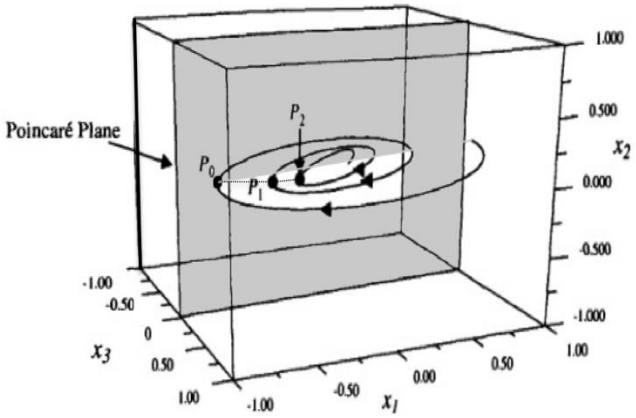

quasiperiodic attractors (dim.2)

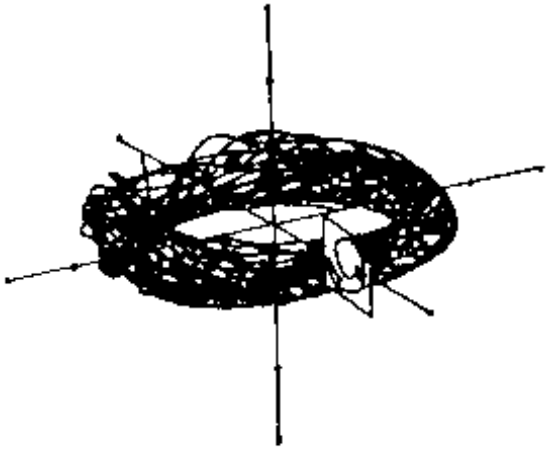

Biforcazioni

1D-2D: Repellor-Node (or Saddle-Node or Tangent) Bifurcation

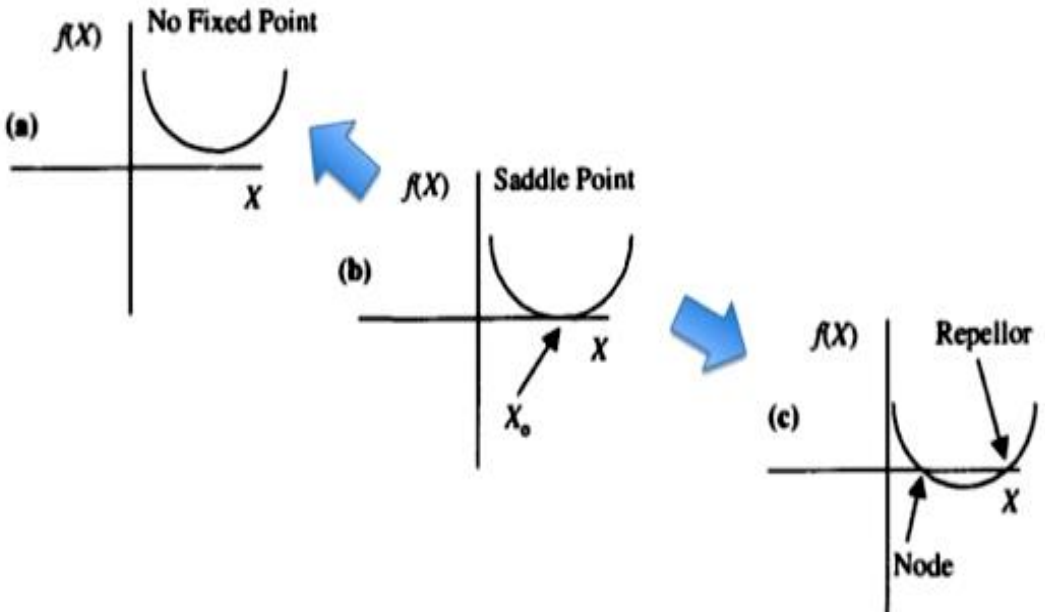

2D: Hopf Bifurcation

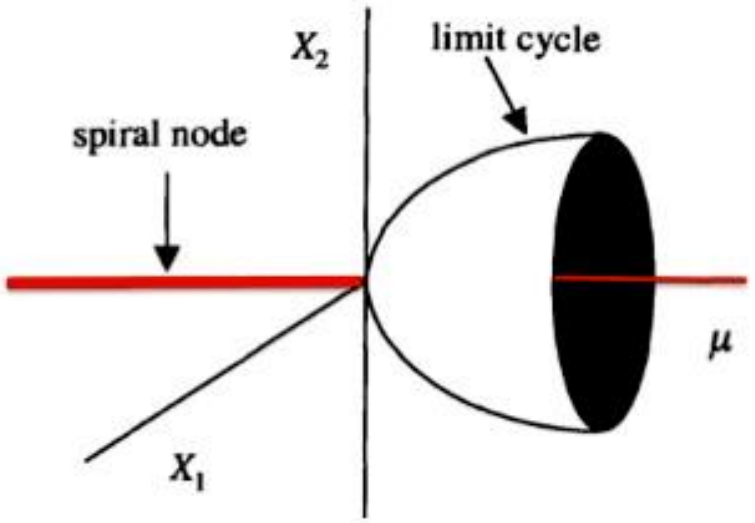

3D: . . . (Rotte verso il Caos…)

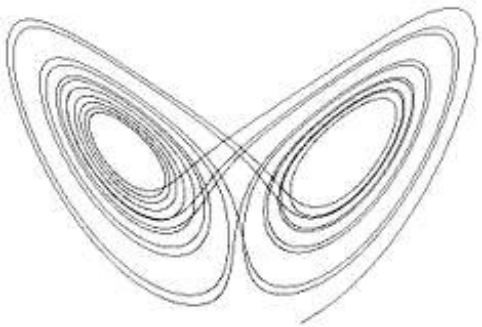

Rotte verso il CAOS...

I : Period-Doubling

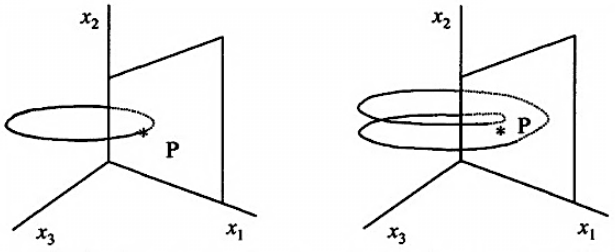

II : Quasi-Periodicity

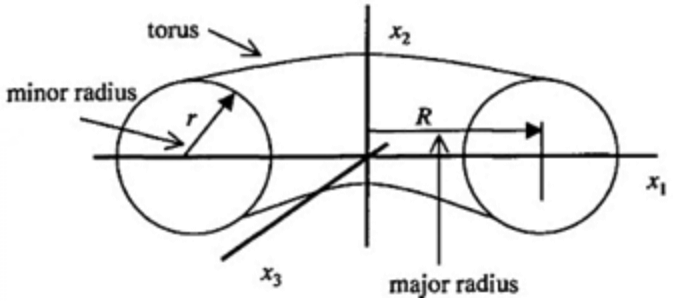

III : Intermittency and Crises

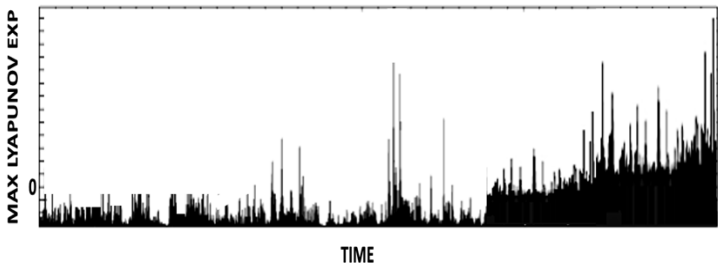

IV : Chaotic Transient and Homoclinic Orbits

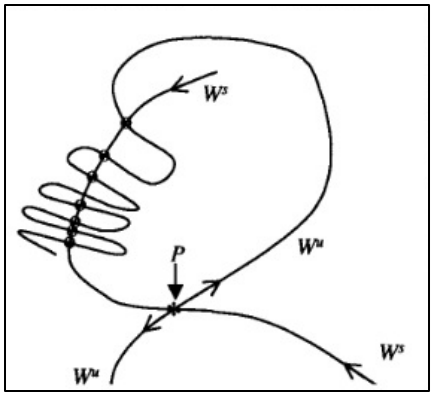

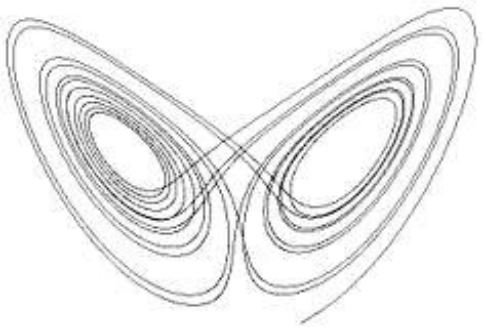

Rotte verso il CAOS...

I : Period-Doubling

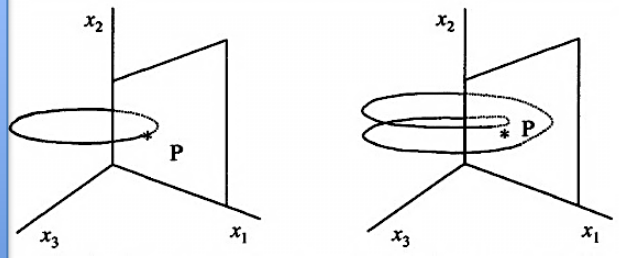

II : Quasi-Periodicity

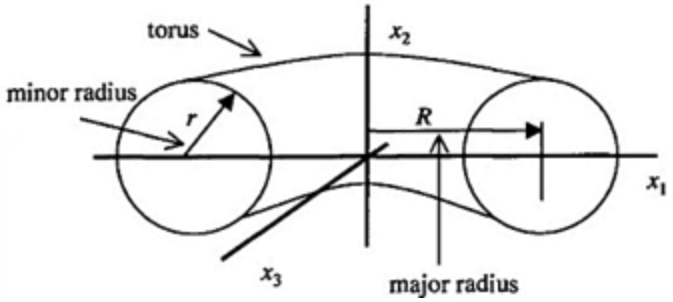

III : Intermittency and Crises

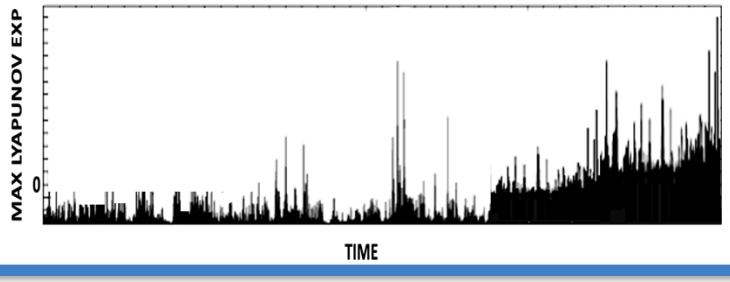

Local Bifurcations

Global Bifurcations

IV : Chaotic Transient and Homoclinic Orbits

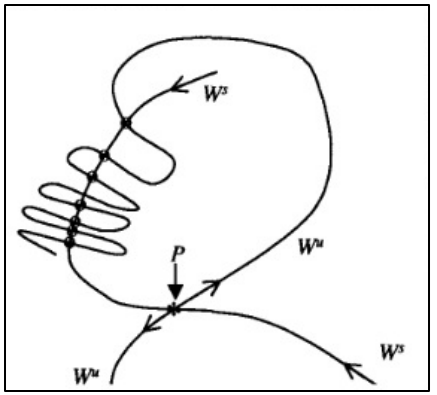

Rotte verso il CAOS

Local Bifurcations

When the parameters of a system are changed, chaotic behavior may appear and disappear in several different ways, even for the same dynamical system: We may have several ***routes to chaos***. These routes can be put into two broad categories with several subdivisions within each category. One category includes sequences of bifurcations involving limit cycles (or equivalently, fixed points of the associated Poincaré map). (The period-doubling sequence in Chapter 1 belongs to this category.) The other category involves changes in trajectories associated with several fixed points or limit cycles. Since these changes involve the properties of trajectories ranging over a significant volume of state space, these changes are called "global" bifurcations (in contrast to "local" bifurcations associated with changes in individual fixed points).

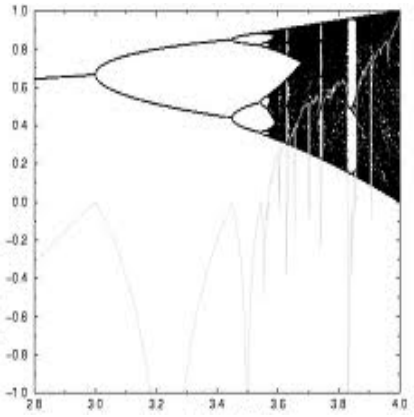

Global Bifurcations

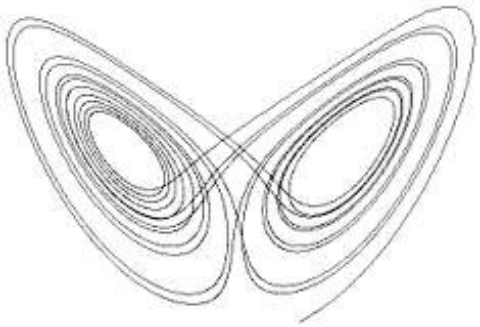

Rather sudden changes from regular to chaotic behavior, such as we have seen with the Lorenz model in Chapter 1, are characteristic of these global bifurcations. Although the nature of the long-time attractor changes suddenly as a parameter is varied, these sudden changes are often heralded by ***chaotic transients***. In a chaotic transient, the system's trajectory wanders through state space, in an apparently chaotic fashion. Eventually, the trajectory approaches a regular, periodic attractor. As the control parameter is changed, the chaotic transient lasts longer and longer until finally the asymptotic behavior is itself chaotic.

The questions we want to address are the following: How does this complicated chaotic behavior develop? How does the system evolve from regular, periodic behavior to chaotic behavior? What changes in the fixed points and in trajectories in state space give rise to these changes in behavior?

I

4.8 The Routes to Chaos I: Period-Doubling

As we discussed earlier, the period-doubling route begins with limit cycle behavior of the system. This limit cycle, of course, may have been "born" from a bifurcation involving a node or other fixed point, but we need not worry about that now. As some control parameter changes, this limit cycle becomes unstable. Again this event is best viewed in the corresponding Poincaré section. Let us assume that the periodic limit cycle generates a single point in the Poincaré section. If the limit cycle becomes unstable by having one of its characteristic multipliers become more negative than -1 (which, of course, means $|M| > 1$), then, in many situations, the new motion remains periodic but has a period twice as long as the period of the original motion. In the Poincaré section, this new limit cycle exhibits two points, one on each side of the original Poincaré section point (see Fig. 4.10).

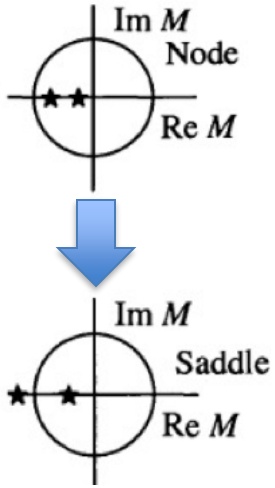

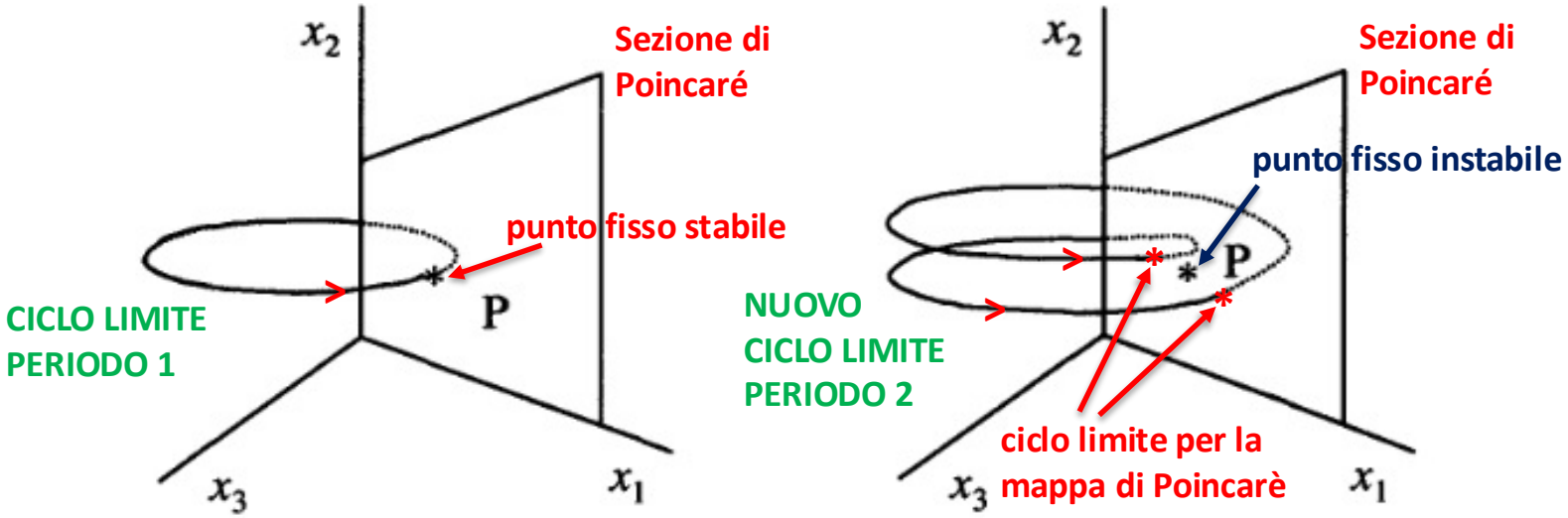

Fig. 4.10. The Poincaré section of a trajectory that has undergone a period-doubling bifurcation. On the left is the original periodic trajectory, which intersects the Poincaré plane in one point. On the right is the period-doubled trajectory, which intersects the Poincaré plane in two points, one on each side of the original intersection point.

mappa 1 dim

$$d_{n+1} = M^n d_1$$

This alternation of intersection points is related to the characteristic multiplier associated with the original limit cycle, which has gotten more negative than −1. Since $|M| > 1$, the trajectory's map points are now being "repelled" by the original map point. The minus sign tells us that they alternate from one side to the other, as we can see formally from Eq. (3.16-6). This type of bifurcation is also called a ***flip bifurcation*** because the newly born trajectory flips back and forth from one side of the original trajectory to the other.

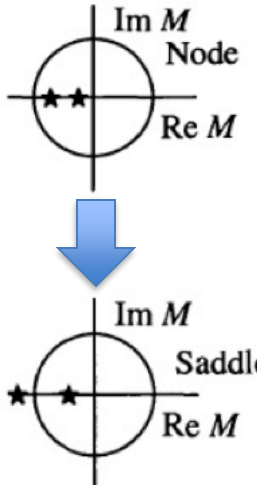

As the control parameter is changed further, this period-two limit cycle may become unstable and give birth to a period-four cycle with four Poincaré intersection points. Chapter 5 will examine in detail how, when, and where this sequence occurs. The period-doubling process may continue until the period becomes infinite; that is, the trajectory never repeats itself. The trajectory is then chaotic.

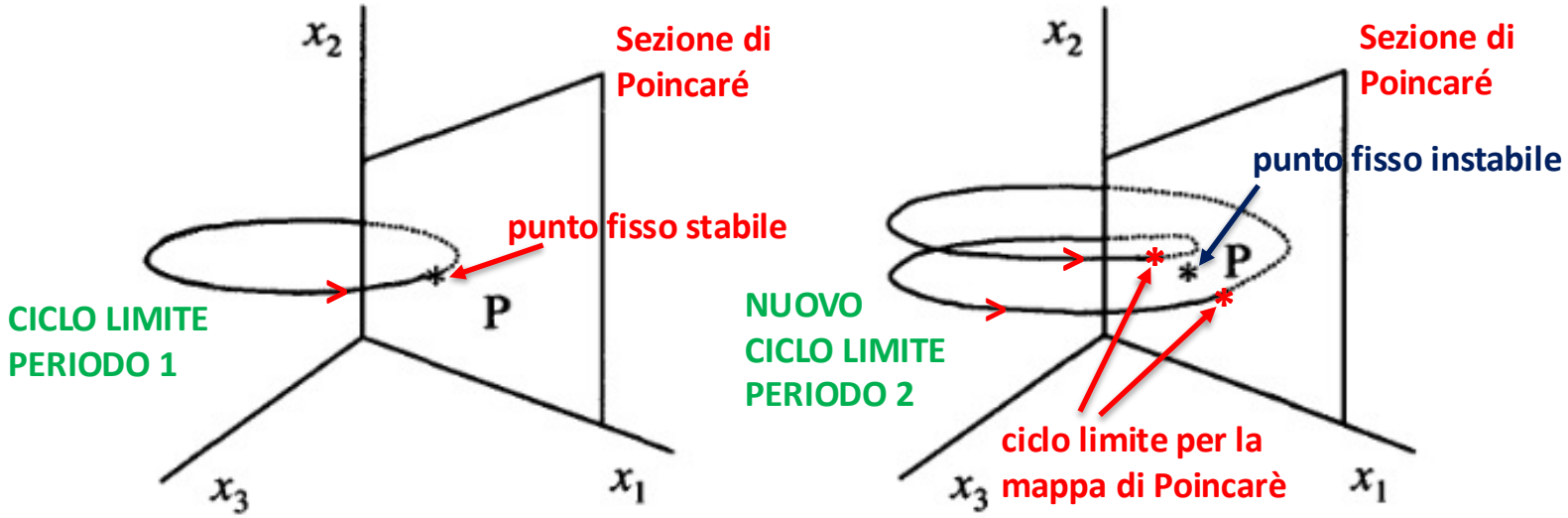

Fig. 4.10. The Poincaré section of a trajectory that has undergone a period-doubling bifurcation. On the left is the original periodic trajectory, which intersects the Poincaré plane in one point. On the right is the period-doubled trajectory, which intersects the Poincaré plane in two points, one on each side of the original intersection point.

II

4.9 The Routes to Chaos II: Quasi-Periodicity

In the quasi-periodic scenario, the system begins again with a limit cycle trajectory. As a control parameter is changed, a second periodicity appears in the behavior of the system. This bifurcation event is a generalization of the ***Hopf bifurcation*** discussed in Chapter 3; so, it is also called a Hopf bifurcation. In terms of the characteristic multipliers, the Hopf bifurcation is marked by having the two complex-conjugate multipliers cross the unit circle simultaneously.

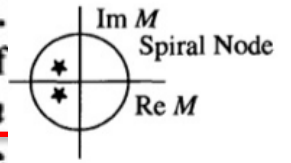

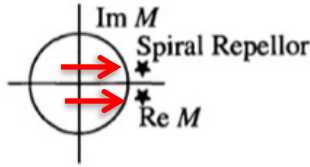

If the ratio of the period of the second type of motion to the period of the first is not a rational ratio, then we say, as described previously, that the motion is quasi-periodic. Under some circumstances, if the control parameter is changed further, the motion becomes chaotic. This route is sometimes called the Ruelle–Takens scenario after D. Ruelle and F. Takens, who in 1971 first suggested the theoretical possibility of this route. The main point here is that you might expect, at first thought, to see a long sequence of different frequencies come in as the control parameter is changed, much like the infinite sequence of period-doublings described in the previous section. (In 1944 the Russian physicist L. Landau had proposed such an infinite sequence of frequencies as a mechanism for producing fluid turbulence. [Landau and Lifshitz, 1959].) However, at least in some cases, the system becomes chaotic instead of introducing a third distinct frequency for its motion. This scenario will be discussed in Chapter 6.


David Ruelle
(1935)


Floris Takens
(1940-2010)

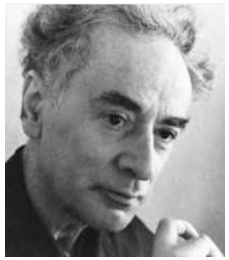
Lev Landau
(1908-1968)

Historically, the experimental evidence for the quasi-periodic route to chaos (GOS75) played an important role in alerting the community of scientists to the utility of many of the newly emerging ideas in nonlinear dynamics. During the late 1970s and early 1980s there were many theoretical conjectures about the necessity of the transition from two-frequency quasi-periodic behavior to chaos. More recent work (see for example, BAT88) has shown that systems with significant spatial extent and with more degrees of freedom can have quasi-periodic behavior with three or more frequencies before becoming chaotic.

III

4.10 The Routes to Chaos III: Intermittency and Crises

Chapter 7 contains a detailed discussion of intermittency and crises; so, we will give only the briefest description here. The intermittency route to chaos is characterized by dynamics with irregularly occurring bursts of chaotic behavior interspersed with intervals of apparently periodic behavior. As some control parameter of the system is changed, the chaotic bursts become longer and occur more frequently until, eventually, the entire time record is chaotic.

A crisis is a bifurcation event in which a chaotic attractor and its basin of attraction suddenly disappear or suddenly change in size as some control parameter is adjusted. Alternatively, if the parameter is changed in the opposite direction, the chaotic attractor can suddenly appear "out of the blue" or the size of the attractor can suddenly be reduced. As we shall see in Chapter 7, a crisis event involves the interaction between a chaotic attractor and an unstable fixed point or an unstable limit cycle.

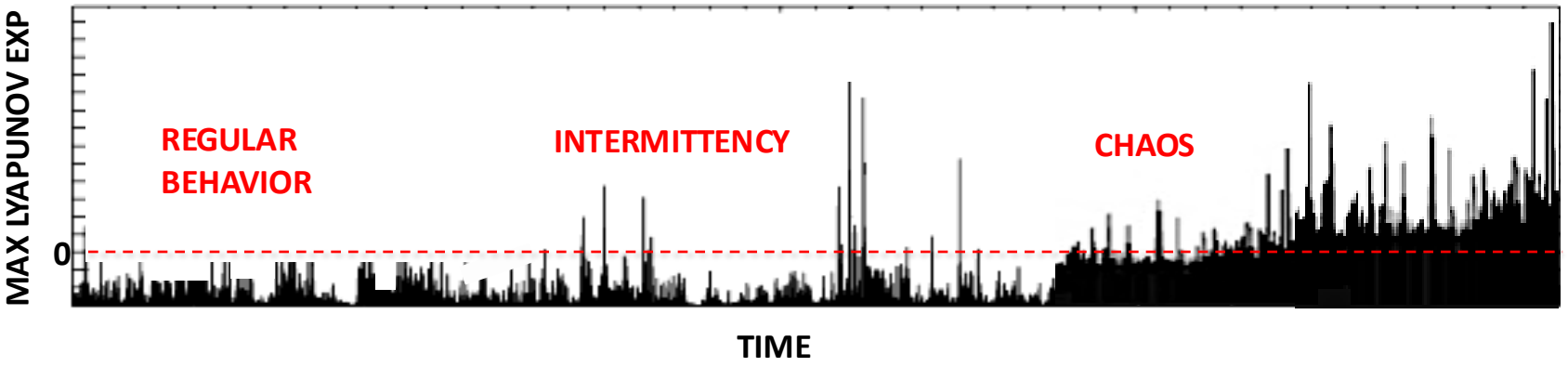

IV

4.11 The Routes to Chaos IV: Chaotic Transients and Homoclinic Orbits

In our second broad category of routes to chaos, the global bifurcation category, the chaotic transient route is the most important for systems modeled by sets of ordinary differential equations. Although the chaotic transient route to chaos was one of the first to be recognized in a model of a physical system (the Lorenz model), the theory of this scenario is, in some ways, less well developed than the theory for period-doubling, quasi-periodicity, and intermittency. This lack of development is due to the fact that this transition to chaos is not (usually) marked by any change in the fixed points of the system or the fixed points of a Poincaré section. The transition is due to the interaction of trajectories with various unstable fixed points and cycles in the state space. The common features are the so-called ***homoclinic*** orbits and their cousins, ***heteroclinic*** orbits. These special orbits may suddenly appear as a control parameter is changed. More importantly, these orbits strongly influence the nature of other trajectories passing near them.

What is a homoclinic orbit? To answer this question, we need to consider *saddle cycles* in a three-dimensional state space. (These ideas carry over in a straightforward fashion to higher-dimensional state spaces.) You should recall that saddle points and saddle cycles and, in particular, their in-sets and out-sets serve to organize the state space. That is, the in-sets and out-sets serve as "boundaries" between different parts of the state space and all trajectories must respect those boundaries. We will focus our attention on a saddle point in the Poincaré section of the state space. This saddle point corresponds to a saddle cycle in the original three-dimensional state space (see Fig. 4.11). We can consider the saddle cycle to be the intersection between two surfaces: One surface is the in-set (that is, the *stable manifold*) associated with the cycle. The other surface is the out-set (*unstable manifold*) associated with the cycle. Trajectories on the in-set approach the saddle cycle as time goes on. Trajectories on the out-set diverge from the cycle as time goes on. Trajectories that are near to, but not on, the in-set will first approach the cycle and then be repelled roughly along the out-set (unstable manifold).

2 dim: saddle point

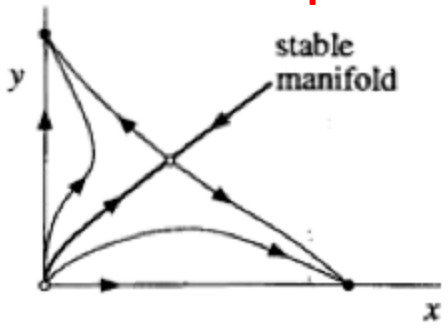

3 dim: saddle cycle

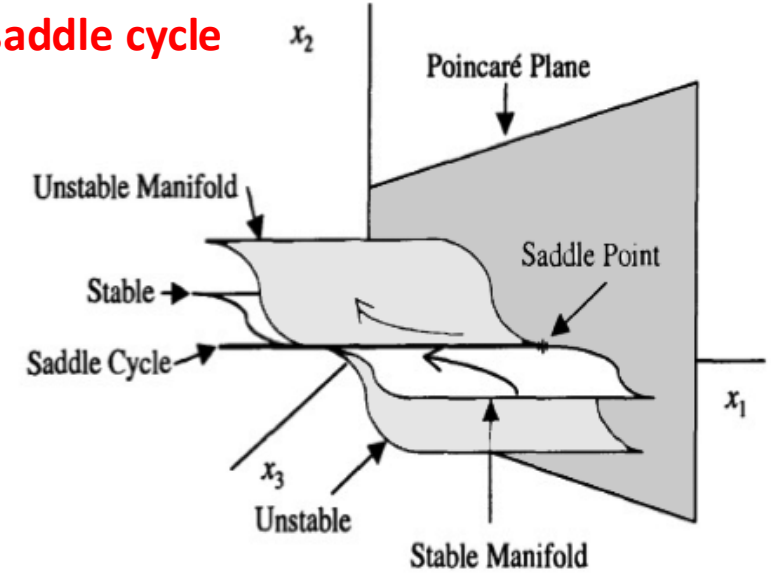

Fig. 4.11. A saddle cycle in a three-dimensional state space. The stable and unstable manifolds are surfaces that intersect at the saddle cycle. Where the saddle cycle intersects a Poincaré plane we have a saddle point for the Poincaré map function. A portion of one trajectory, repelled by the saddle cycle, is shown on the unstable manifold, and a portion of another trajectory, approaching the saddle cycle, is shown on the stable manifold.

Fig. 4.12 shows the equivalent Poincaré section with a saddle point P where the saddle cycle intersects the plane. We have sketched in some curves to indicate schematically where the in-set and out-set surfaces cut the Poincaré plane. These curves, labeled $W^s(P)$ and $W^u(P)$, are called the *stable* and *unstable manifolds* of the saddle point P. Since the in-set and out-set of a saddle cycle are generally two-dimensional surfaces (in the original three-dimensional state space), the intersection of one of these surfaces with the Poincaré plane forms a curve. It is crucial to realize that these curves are not trajectories. For example, if we pick a point s_0 on $W^s(P)$, a point at which some trajectory intersects the Poincaré plane, then the Poincaré map function F gives us s_1, the coordinates of the point at which the trajectory next intersects the plane. From s_1, we can find s_2, and so on. The sequence of points lies along the curve labeled $W^s(P)$ and approaches P as $n \to \infty$. Similarly, if u_0 is a point along $W^u(P)$, then $F(u_0) = u_1$, $F(u_1) = u_2$, and so on, generates a series of points that diverges from P along $W^u(P)$. If we apply the inverse of the Poincaré map function $F^{(-1)}$ to u_0, we generate a sequence of points u_{-1}, u_{-2}, and so on, that approaches P as $n \to -\infty$. The curves drawn in Fig. 4.12 represent the totality of such sequences of points taken with infinitely many starting points. For any one starting point, however, the sequence jumps along W^s or W^u, it does not move smoothly like a point on a trajectory in the original state space.

Sezione di Poincarè

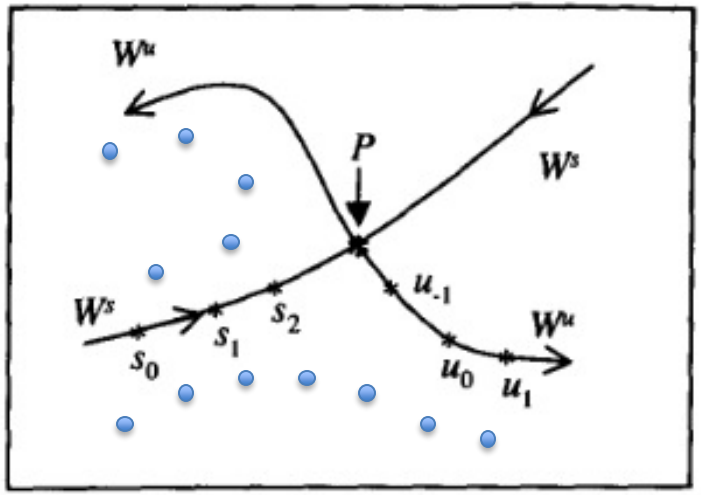

Fig. 4.12. Point P is a saddle point in a Poincaré section. It corresponds to a saddle cycle in the full three-dimensional state space. The intersection of the in-set of the saddle cycle with the Poincaré plane generates the curve labeled W^s. The intersection of the out-set of the saddle cycle with the Poincaré plane generates curve W^u.

As a control parameter is changed, it is possible for $W^s(P)$ and $W^u(P)$ to approach each other and in fact to intersect, say, at some point q. If this intersection occurs, we say that we have a ***homoclinic intersection*** at q, and the point q is called a ***homoclinic (intersection) point***. It is also possible for the unstable manifold of one saddle point to intersect the stable manifold from some other saddle point. In that case we say we have a ***heteroclinic intersection***. Other heteroclinic combinations are possible. For example, we could have the intersection of the unstable manifold surface of an index-2 saddle point and the stable manifold of a saddle cycle. (For a nice visual catalog of the possible kinds of intersections, see [Abraham and Shaw, 1992][Abraham, Abraham, and Shaw, 1996].) For now we will concentrate on homoclinic intersections.

We now come to an important and crucial theorem:

homoclinic intersection

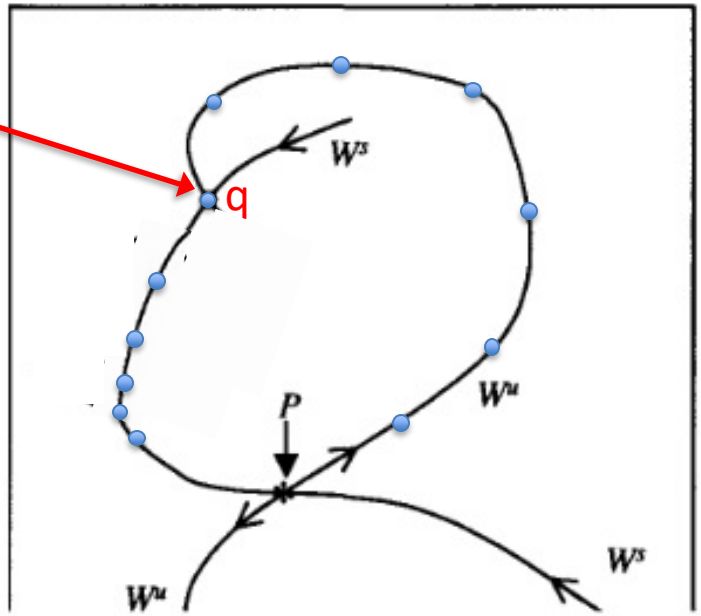

Fig. 4.13. A homoclinic tangle results from the homoclinic intersection of the unstable manifold $W^u(P)$ with the stable manifold $W^s(P)$ of the saddle point P. Each of the circled points is a homoclinic (intersection) point. For clarity's sake, only a portion of the tangle is shown.

TEOREMA

> If the in-sets and out-sets of a saddle point in the Poincaré section of a dynamical system intersect at one homoclinic intersection point q_0, then there must be an infinite number of homoclinic intersections.

To prove this statement, we consider the result of applying the mapping function F to q_0. We get another point q_1. Since q_0 belongs to both W^s and W^u, so must q_1, since we have argued in the previous paragraphs that applying F to a point on W^s or W^u generates another point on W^s or W^u. By continuing to apply F to this sequence of points, we generate an infinite number of homoclinic points. Fig. 4.13 shows part of the resulting *homoclinic tangle*, which must result from the homoclinic intersections.

Please note that the smooth curves drawn in Fig. 4.13 are not individual trajectories. (We cannot violate the No-Intersection Theorem!) The smooth curves are generated by taking infinitely many starting points on W^s and W^u. Only those trajectories that hit one of the homoclinic points will hit (some of) the other homoclinic points.

homoclinic tangle

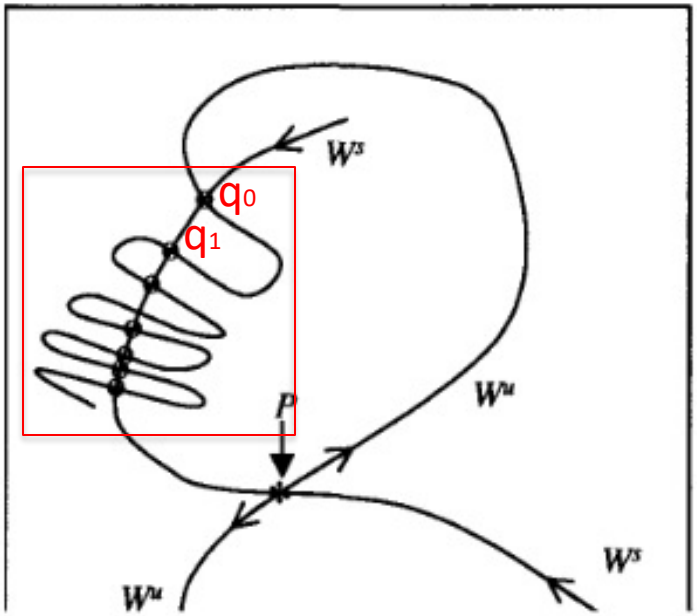

Fig. 4.13. A homoclinic tangle results from the homoclinic intersection of the unstable manifold $W^u(P)$ with the stable manifold $W^s(P)$ of the saddle point P. Each of the circled points is a homoclinic (intersection) point. For clarity's sake, only a portion of the tangle is shown.

What is the dynamical significance of a homoclinic point and the related homoclinic tangle? If we now shift our attention back to the original three-dimensional state space, we see that a homoclinic point in the Poincaré section corresponds to a continuous trajectory in the original state space. When a homoclinic intersection occurs, one trajectory on the unstable manifold joins another trajectory on the stable manifold to form a single new trajectory whose Poincaré intersection points are the homoclinic points described earlier. (To help visualize this process, recall that the in-set and out-set of a saddle cycle in the three-dimensional state space are, in general, two-dimensional surfaces.) This new trajectory connects the saddle point to itself and hence is called a ***homoclinic trajectory*** or ***homoclinic orbit*** and is said to form a ***homoclinic connection***. As our previous theorem states, this homoclinic trajectory must intersect the Poincaré plane an infinite number of times.

Sezione di Poincarè

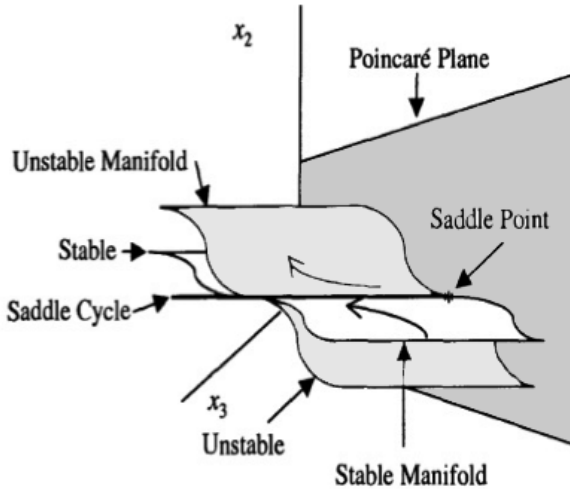

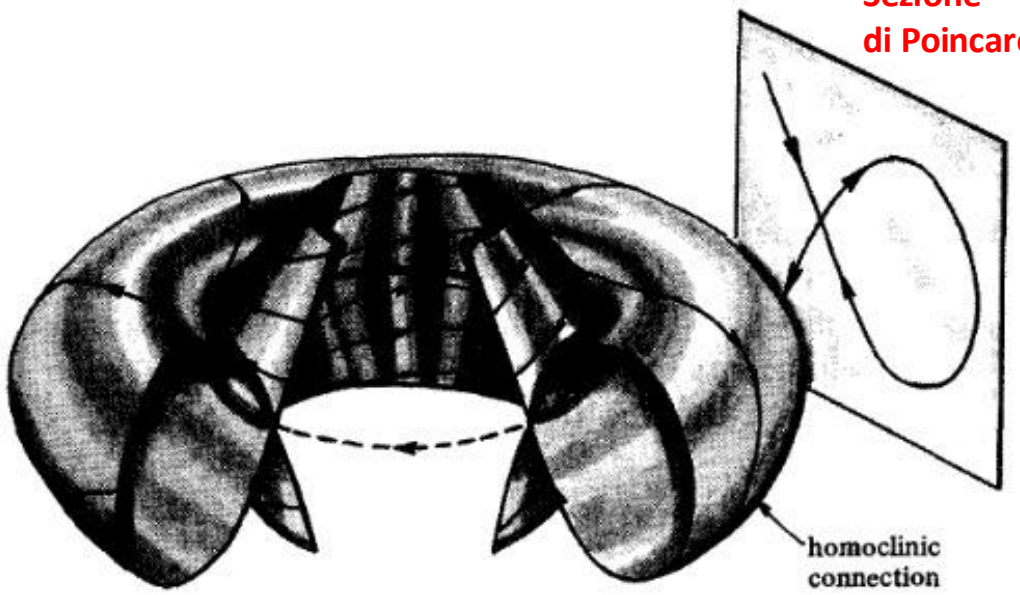

(a)

How does a homoclinic orbit lead to chaotic behavior? To understand this, we need to consider other trajectories that come near the saddle point of the Poincaré section. Generally speaking, the trajectories approach the saddle point close to (but not on) the in-set (stable manifold), but they are then forced away from the saddle point near the out-set (unstable manifold). After a homoclinic tangle has developed, a trajectory will be pushed away from the saddle point by the out-set part of the tangle, but it will be pulled back by the in-set part. It is easy to see that the homoclinic tangle can lead to trajectories that seem to wander randomly around the state space region near the saddle point.

Sezione di Poincarè

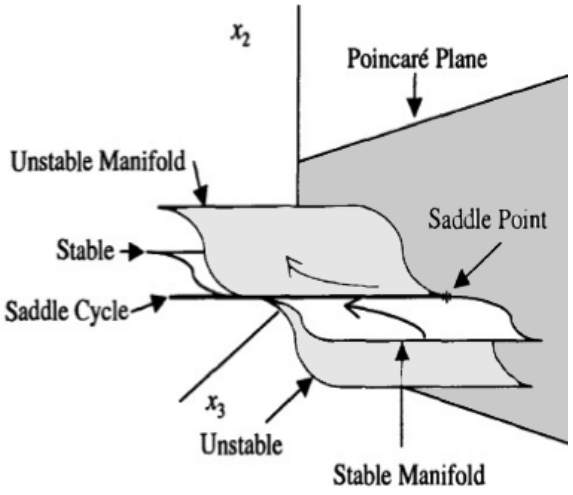

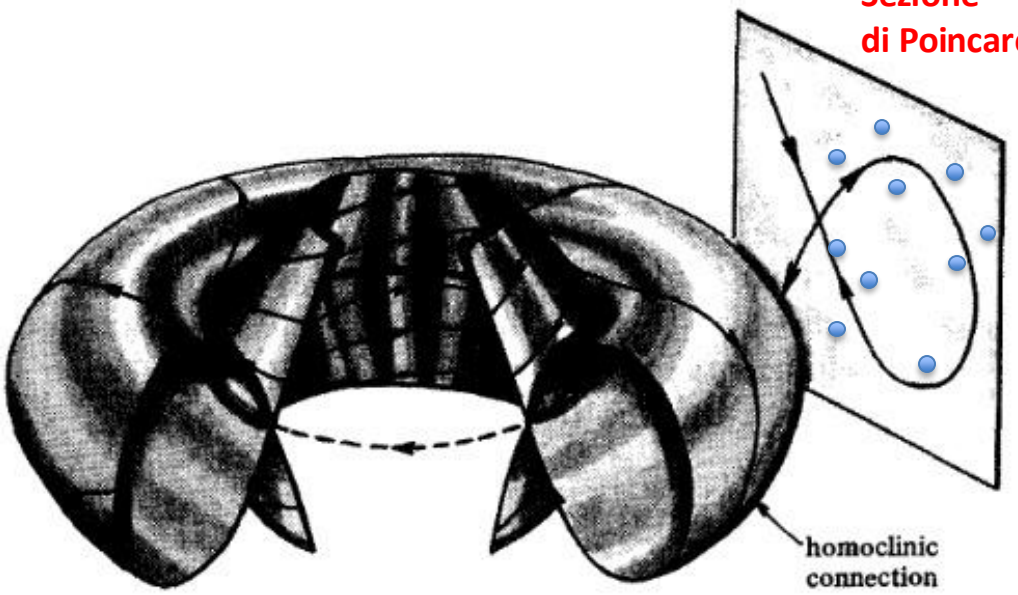

(a)

The same general type of behavior can result from a ***heteroclinic orbit***, which connects one saddle point (or saddle cycle in the original state space) to another. A second heteroclinic orbit takes us from the second saddle point back to the first. When such a combined trajectory exists, we say we have a ***heteroclinic connection*** between the two saddle cycles. Figure 4.14 shows schematically a part of a heteroclinic connection in a Poincaré section of a three-dimensional state space. It is also possible to have heteroclinic orbits that link together sequentially three or more saddle cycles.

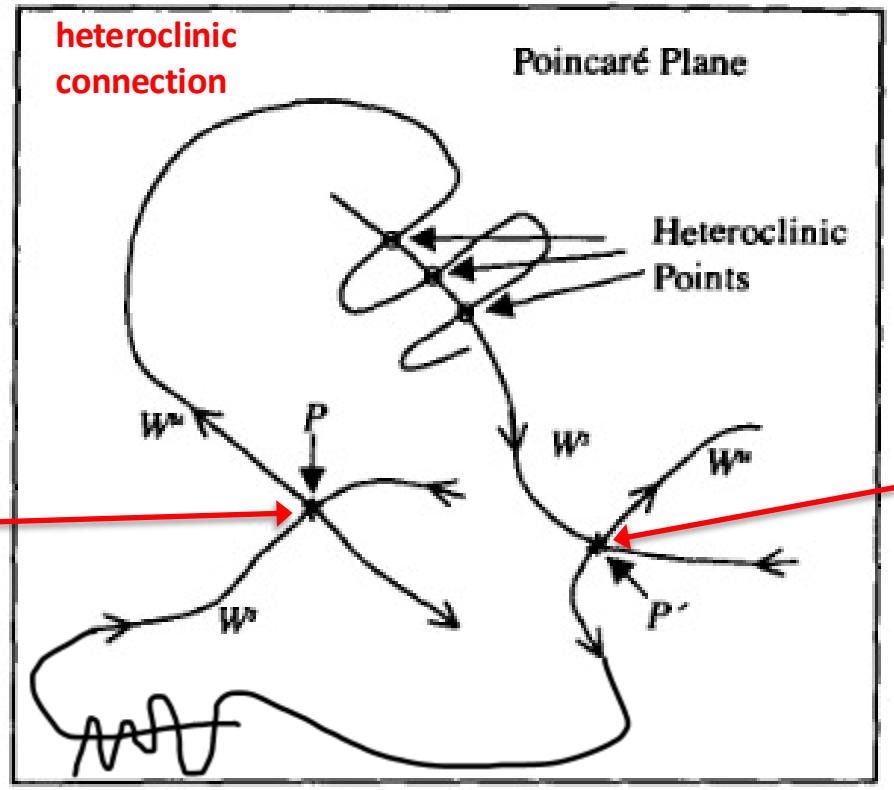

Fig. 4.14. The Poincaré section of a heteroclinic connection. Two saddle cycles intersect the plane at P and P' respectively. A heteroclinic orbit links together two saddle cycles forming a heteroclinic connection. For the sake of clarity only the part of the tangle involving the unstable manifold of P intersecting the stable manifold of P' is shown

Saddle point P corrispondente al primo saddle cycle

Saddle point P' corrispondente al secondo saddle cycle

heteroclinic

connections in three-dimensional state spaces for which the in-sets and out-sets of a saddle cycle are two-dimensional surfaces. Also shown are partial pictures of the resulting Poincaré sections.

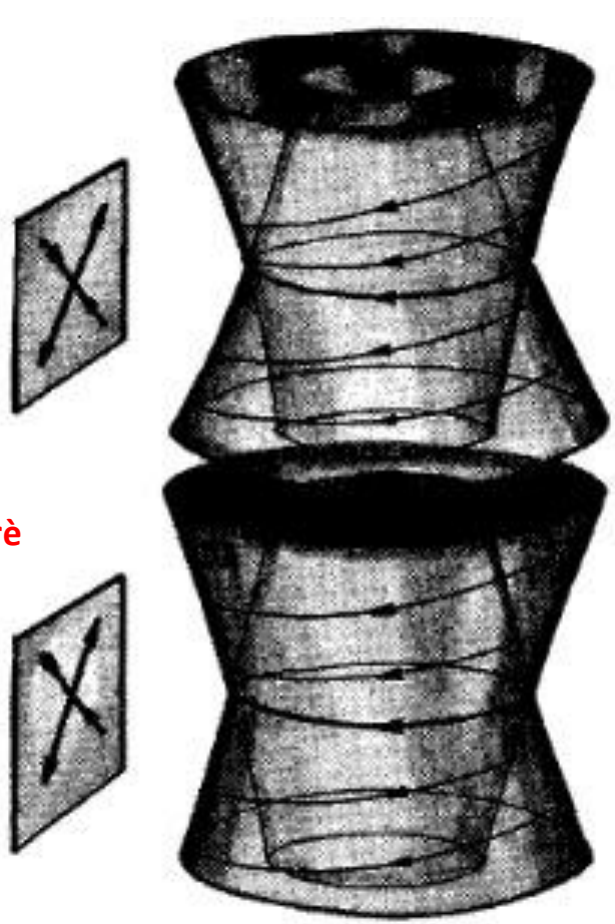

Sezioni
di Poincarè

(b)

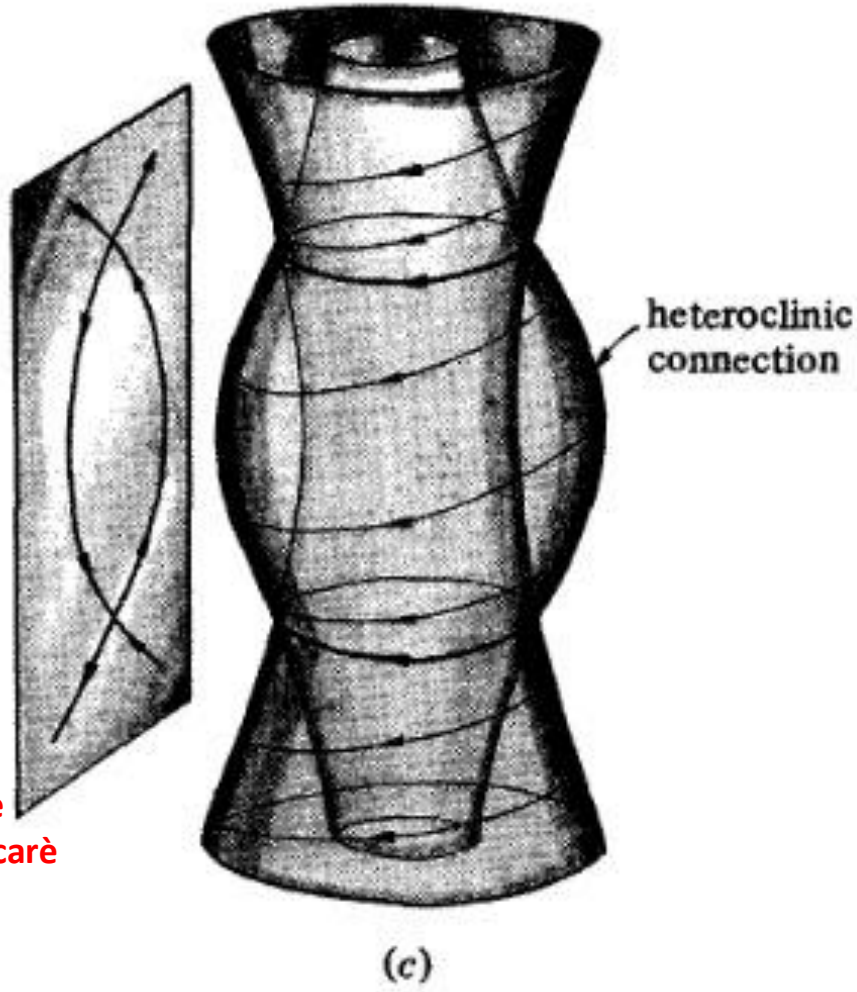

Sezione
di Poincarè

(c)

Figure 4.16 shows three-dimensional constructions of homoclinic and heteroclinic tangles resulting from the intersections of the in-sets and out-sets of saddle cycles. Partial diagrams of the corresponding Poincaré sections are also shown.

Homoclinic connection

Sezioni di Poincarè

Heteroclinic connection

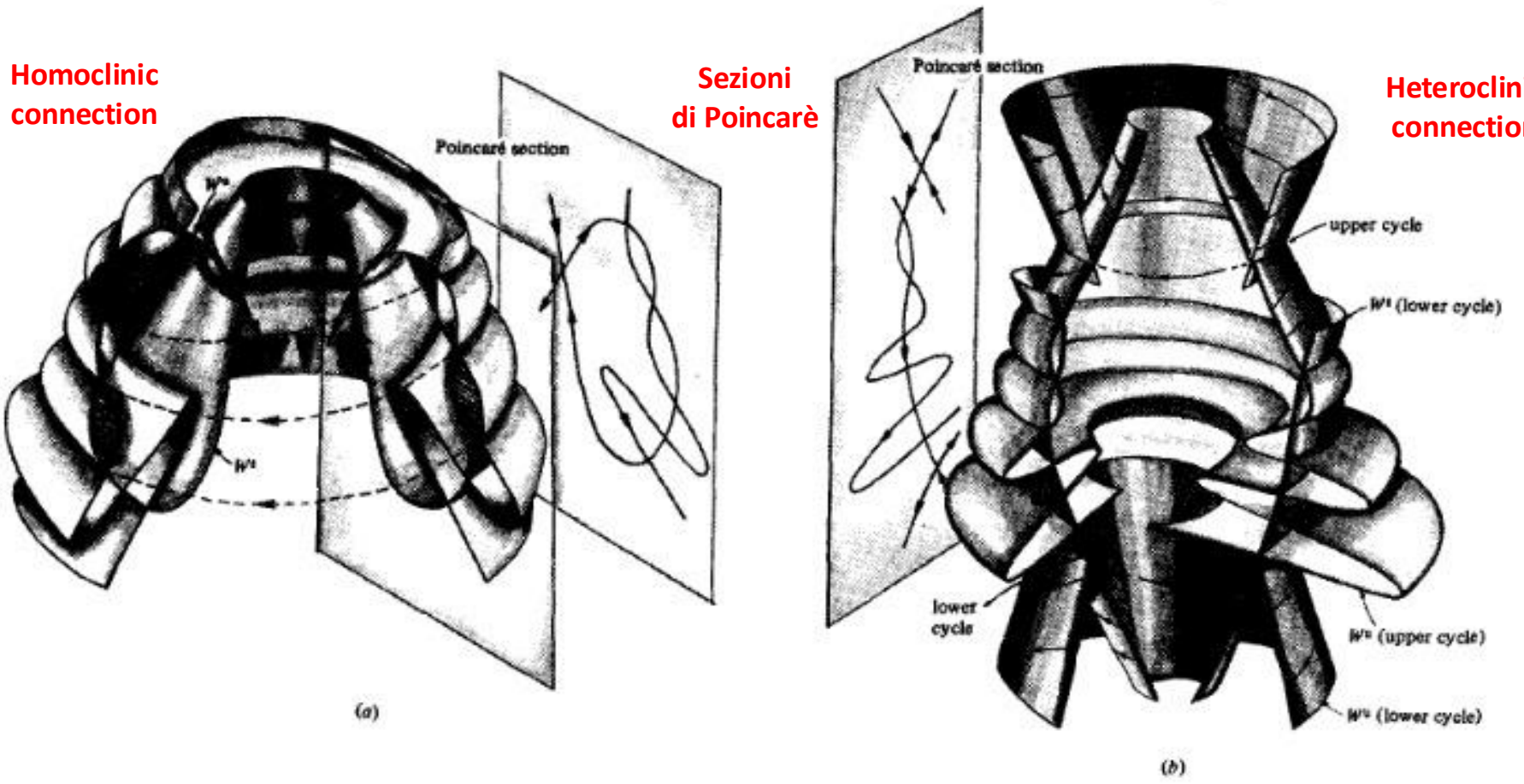

Così, nel terzo volume del suo *Méthodes nouvelles de la mécanique céleste* (1882-1889), lo stesso **Poincarè** descrisse la scoperta del «tangle» omoclinico compiuta mentre cercava di risolvere il problema dei tre corpi (un asteroide lanciato nel campo gravitazionale del Sole e di Giove) per mezzo della sua «sezione» (non avendo all'epoca i computer, ovviamente non poté mai visualizzarla...):

«Tentiamo di farci un'idea della figura formata da queste due curve e delle loro intersezioni, che sono in numero infinito e corrispondono ciascuna a una soluzione doppiamente asintotica; queste intersezioni formano una sorta di reticolo, di ordito, di rete dalle maglie infinitamente fitte; ciascuna delle due curve non deve mai intersecare se stessa, ma deve ripiegarsi su se stessa in maniera assai complicata per poter intersecare un'infinità di volte tutte le maglie della rete».

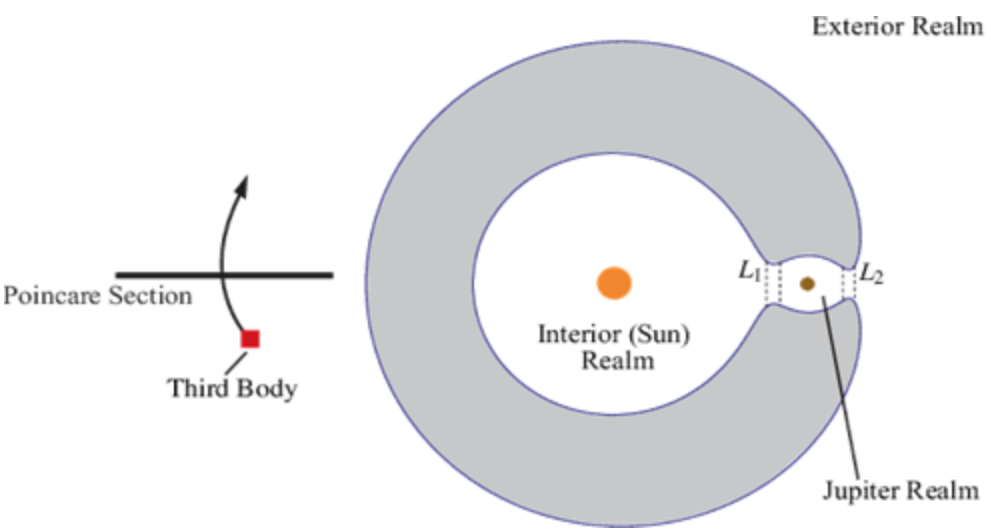

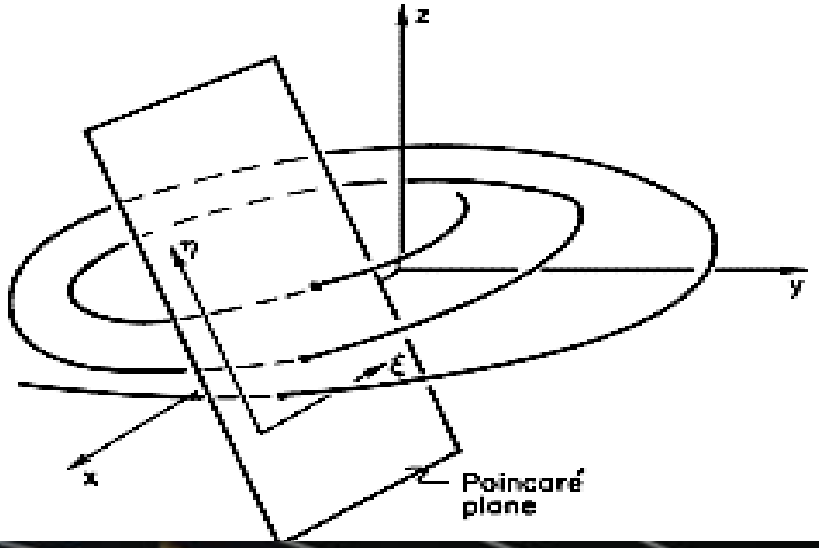

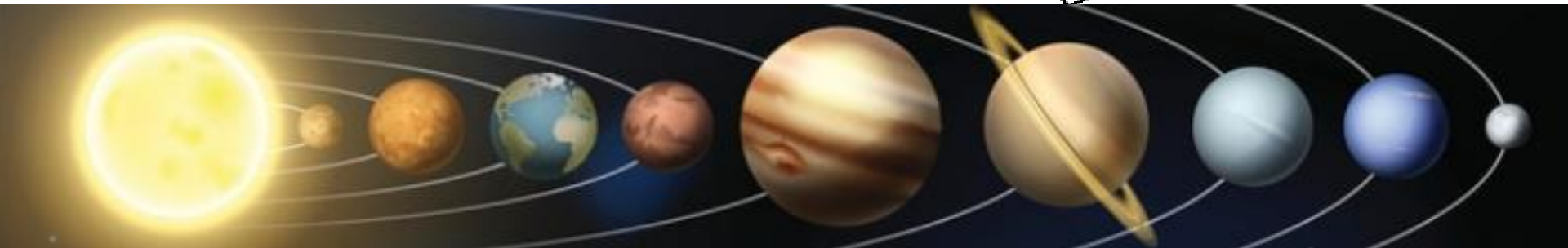

Così, nel terzo volume del suo *Méthodes nouvelles de la mécanique céleste* (1882-1889), lo stesso **Poincarè** descrisse la scoperta del «tangle» omoclinico compiuta mentre cercava di risolvere il problema dei tre corpi (un asteroide lanciato nel campo gravitazionale del Sole e di Giove) per mezzo della sua «sezione» (non avendo all'epoca i computer, ovviamente non poté mai visualizzarla...):

«Tentiamo di farci un'idea della figura formata da queste due curve e delle loro intersezioni, che sono in numero infinito e corrispondono ciascuna a una soluzione doppiamente asintotica; queste intersezioni formano una sorta di reticolo, di ordito, di rete dalle maglie infinitamente fitte; ciascuna delle due curve non deve mai intersecare se stessa, ma deve ripiegarsi su se stessa in maniera assai complicata per poter intersecare un'infinità di volte tutte le maglie della rete».

Per approfondimenti: https://www.vitapensata.eu/2022/01/04/tre-corpi-al-margine-del-caos/

(Tre) corpi al margine del caos

Di: **Alessandro Pluchino**
4 Gennaio 2022

Come è noto, il Tre è spesso considerato il *numero perfetto* da diversi punti di vista: dal punto di vista *matematico* costituisce la sintesi del pari (due) e del dispari (uno); dal punto di vista *esoterico* è il simbolo della Grande Triade (Cielo, Terra, Uomo); infine, dal punto di vista *religioso*, rappresenta la perfezione divina (si pensi alla Trinità del Cristianesimo o alla Trimurti induista). Pochi forse sanno, però, che allo stesso tempo il tre rappresenta anche la *soglia dell'imperfezione*, il numero magico che ha condotto la fisica moderna al confine tra ordine e disordine, in quella strana regione oggi conosciuta come "Margine del Caos", spalancando così le porte alla nuova Scienza della Complessità. E la scintilla da cui questa rivoluzione concettuale è partita riguardava un problema di corpi. Per la precisione, appunto, di tre corpi.

Tutto cominciò la notte tra il 31 agosto e il primo settembre del 1879 in una miniera di carbone di Magny, nella Borgogna francese. Alle 3.45 circa del mattino un'esplosione improvvisa scosse la miniera, ustionando e uccidendo gran parte della squadra di ventidue minatori che si trovavano al lavoro a quell'ora. Fu soltanto la perizia e l'acume scientifico di un giovane ingegnere incaricato delle indagini a permettere di risalire alla causa prima dell'esplosione: si era trattato di una lampada perforata accidentalmente che aveva lasciato uscire la fiamma da cui poi, a contatto con un'atmosfera ricca di metano come quella della miniera, aveva avuto inizio il processo che avrebbe portato alla conflagrazione. Quel giovane ingegnere, appena venticinquenne, si chiamava Jules-Henri Poincaré, colui che più avanti si sarebbe distinto come uno dei più grandi matematici e fisici di fine Ottocento (all'epoca si poteva essere ingegnere, matematico e fisico allo stesso tempo!) e che è considerato oggi uno dei padri della teoria dei sistemi dinamici e il precursore assoluto della moderna teoria del Caos. Sarà lui il principale protagonista della storia che stiamo per raccontarvi.

Così, nel terzo volume del suo *Méthodes nouvelles de la mécanique céleste* (1882-1889), lo stesso **Poincarè** descrisse la scoperta del «tangle» omoclinico compiuta mentre cercava di risolvere il problema dei tre corpi (un asteroide lanciato nel campo gravitazionale del Sole e di Giove) per mezzo della sua «sezione» (non avendo all'epoca i computer, ovviamente non poté mai visualizzarla...):

«Tentiamo di farci un'idea della figura formata da queste due curve e delle loro intersezioni, che sono in numero infinito e corrispondono ciascuna a una soluzione doppiamente asintotica; queste intersezioni formano una sorta di reticolo, di ordito, di rete dalle maglie infinitamente fitte; ciascuna delle due curve non deve mai intersecare se stessa, ma deve ripiegarsi su se stessa in maniera assai complicata per poter intersecare un'infinità di volte tutte le maglie della rete».

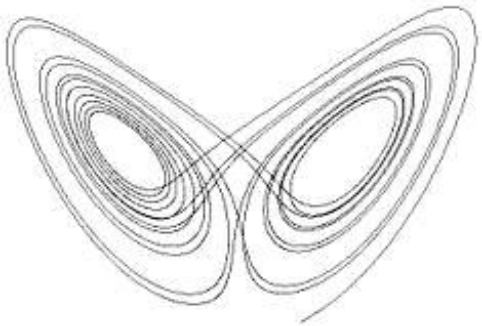

Rotte verso il CAOS...

IL MODELLO DI LORENZ

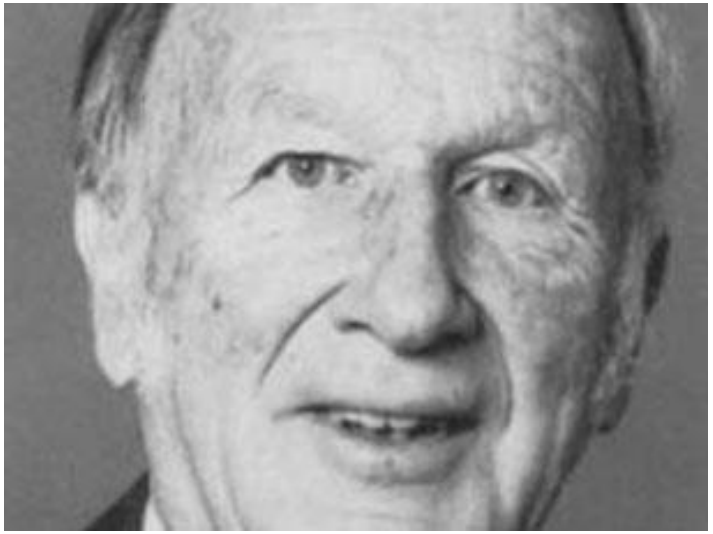

The Lorenz Equations

The Lorenz model is based on a (gross) simplification of the fundamental Navier–Stokes equations for fluids. As shown in Appendix C, the fluid motion and resulting temperature differences can be expressed in terms of three variables, conventionally called $X(t)$, $Y(t)$, and $Z(t)$.

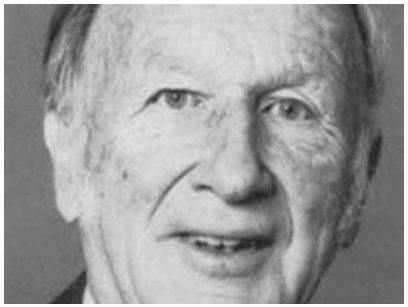

$$\begin{cases} \dot{X} = p(Y - X) \\ \dot{Y} = -XZ + rX - Y \\ \dot{Z} = XY - bZ \end{cases}$$

Riproducono la dinamica delle Celle Convettive di Rayleigh-Bénard

generate dalla differenza di temperatura tra la superficie inferiore e quella superiore del recipiente contenente il fluido

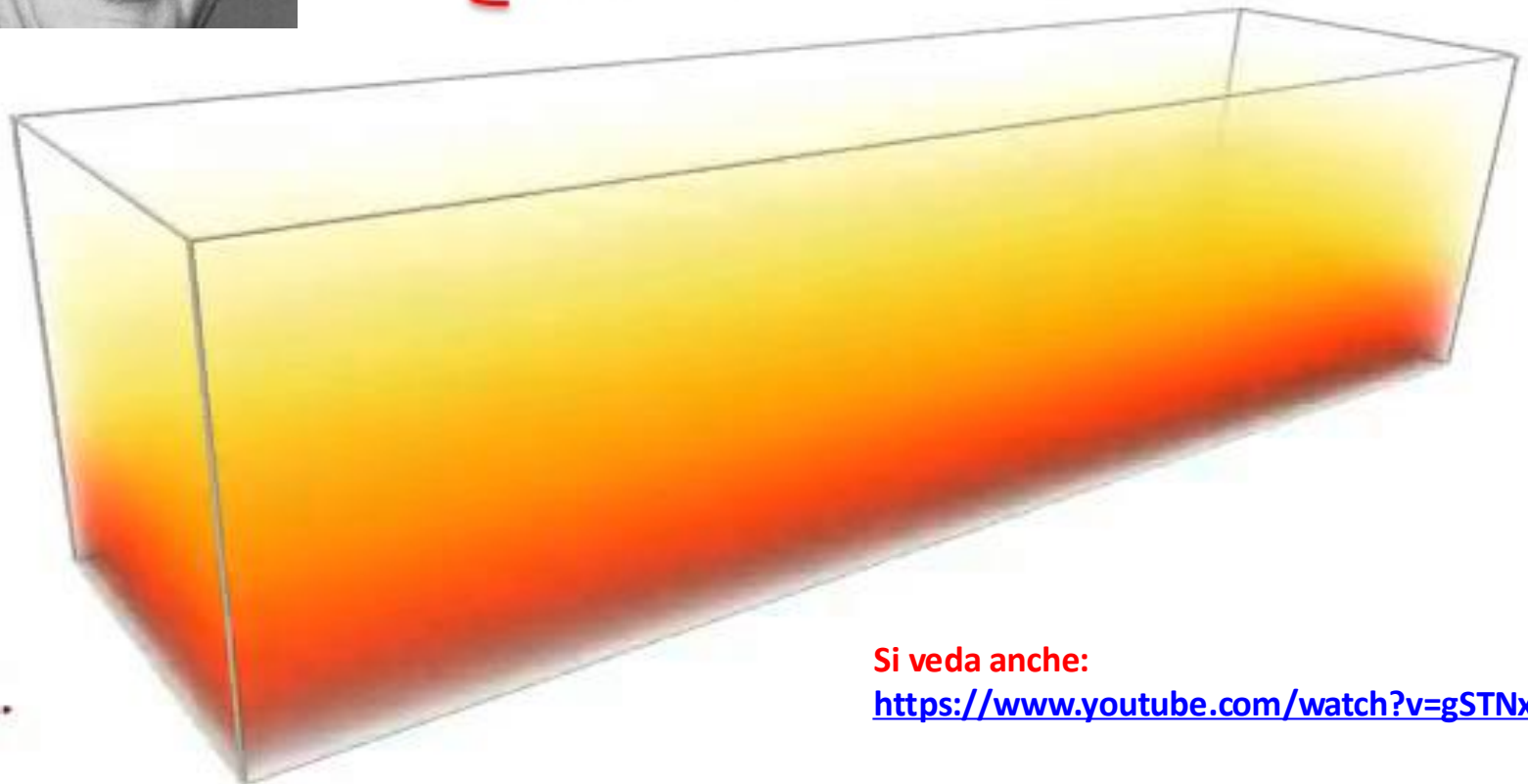

Si veda anche:
https://www.youtube.com/watch?v=gSTNxS96fRg

The Lorenz Equations

The Lorenz model is based on a (gross) simplification of the fundamental Navier–Stokes equations for fluids. As shown in Appendix C, the fluid motion and resulting temperature differences can be expressed in terms of three variables, conventionally called $X(t)$, $Y(t)$, and $Z(t)$.

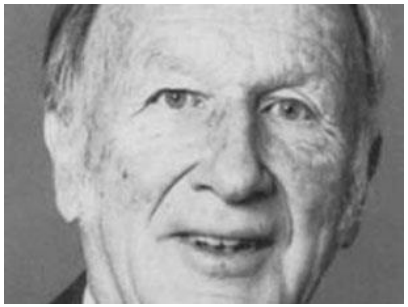

$$\begin{cases} \dot{X} = p(Y - X) \\ \dot{Y} = -XZ + rX - Y \\ \dot{Z} = XY - bZ \end{cases}$$

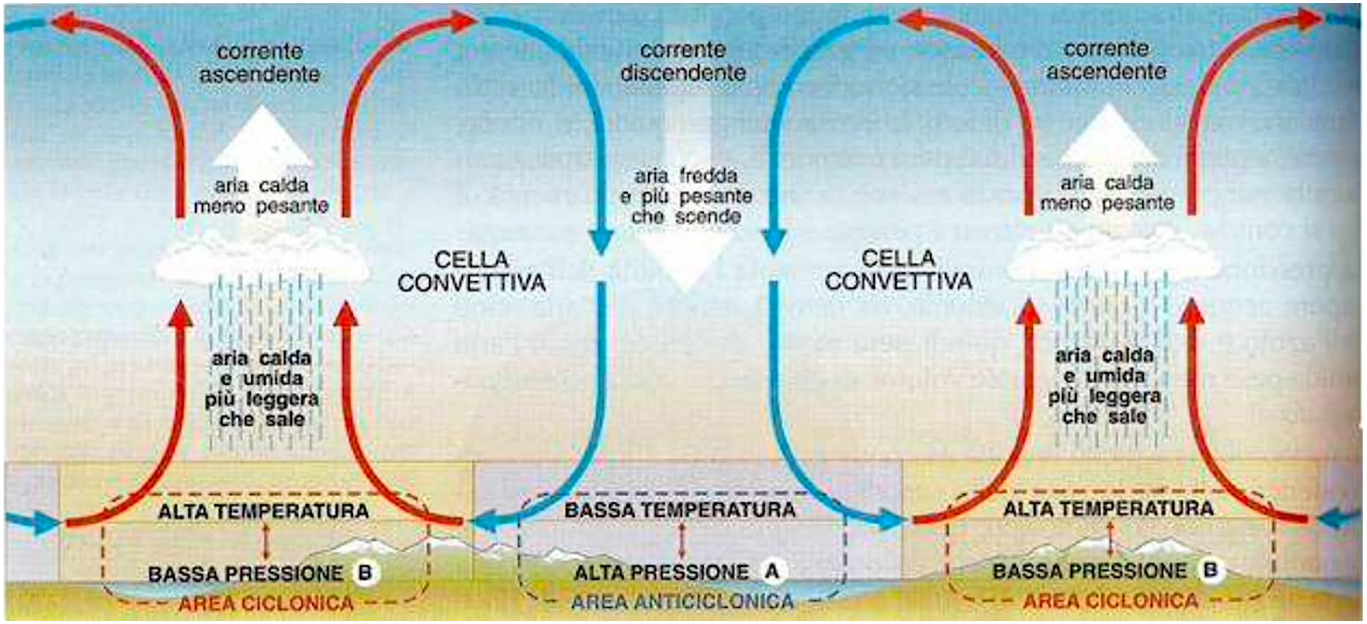

Significato delle 3 variabili:

X(t): dipendenza temporale della funzione di flusso del fluido (le cui derivate rispetto alle variabili spaziali rappresentano le componenti della velocità del fluido)

Y(t): dipendenza temporale della differenza di temperatura tra la parte ascendente e quella discendente del fluido

Z(t): dipendenza temporale della deviazione dalla linearità della temperatura in funzione della posizione verticale

The Lorenz Equations

The Lorenz model is based on a (gross) simplification of the fundamental Navier–Stokes equations for fluids. As shown in Appendix C, the fluid motion and resulting temperature differences can be expressed in terms of three variables, conventionally called $X(t)$, $Y(t)$, and $Z(t)$.

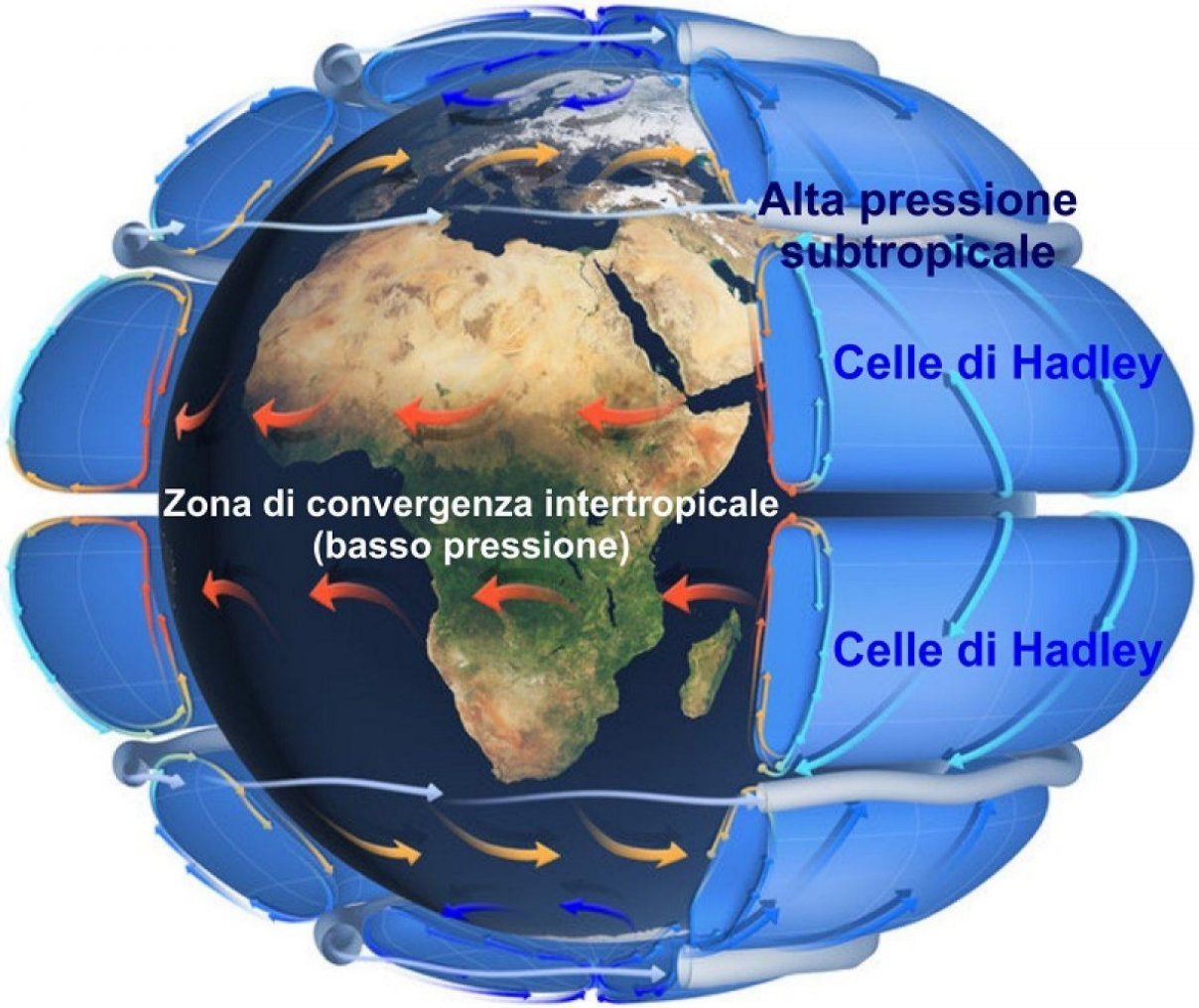

Significato delle 3 variabili:

X(t): dipendenza temporale della funzione di flusso del fluido (le cui derivate rispetto alle variabili spaziali rappresentano le componenti della velocità del fluido)

Y(t): dipendenza temporale della differenza di temperatura tra la parte ascendente e quella discendente del fluido

Z(t): dipendenza temporale della deviazione dalla linearità della temperatura in funzione della posizione verticale

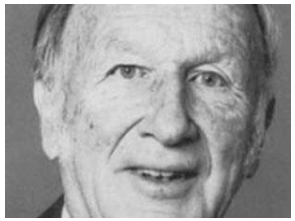

$$\begin{cases} \dot{X} = p(Y - X) \\ \dot{Y} = -XZ + rX - Y \\ \dot{Z} = XY - bZ \end{cases}$$

Significato dei 3 parametri di controllo:

Prandtl number p:
rapporto tra la viscosità cinetica del fluido e il coefficiente di diffusione termica

Rayleigh number r:
misura della differenza di temperatura tra la parte superiore e quella inferiore del fluido

Parameter b:
esprime il rapporto tra l'altezza verticale dello strato di fluido e la dimenzione orizzontale delle celle convettive

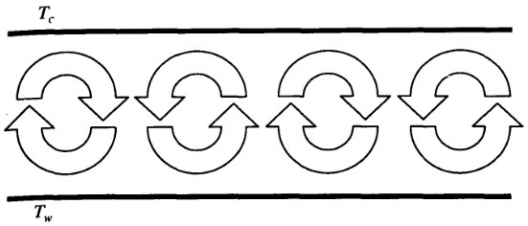

p, r, and b are adjustable parameters; p is the so-called Prandtl number, which is defined to be the ratio of the kinetic viscosity of the fluid to its thermal diffusion coefficient. In rough terms, the Prandtl number compares the rate of energy loss from a small "packet" of fluid due to viscosity (friction) to the rate of energy loss from the packet due to thermal conduction. r is proportional to the ***Rayleigh number***, which is a dimensionless measure of the temperature difference between the bottom and top of the fluid layer. As the temperature difference increases, the Rayleigh number increases. The final parameter b is related to the ratio of the vertical height h of the fluid layer to the horizontal size of the convection rolls. It turns out that for $b = 8/3$, the convection begins for the smallest value of the Rayleigh number, that is, for the smallest value of the temperature difference δT.

This is the value usually chosen for the study of the Lorenz model. p is then chosen for the particular fluid under study. Lorenz (LOR63) used the value $p = 10$ (which corresponds roughly to cold water), a value that had been used in a previous study of Rayleigh–Bénard convection by Saltzman (SAL62). We let r, the Rayleigh number, be the adjustable control parameter.

The Lorenz model, although based on what appears to be a very simple set of differential equations, exhibits very complex behavior. The equations look so simple that one is led to guess that it would be easy to write down their solutions, that is, to give X, Y, and Z as functions of time. In fact, as we shall discuss later, it is now believed that it is in principle impossible to give the solutions in analytic form, that is, to write down a formula that would give X, Y, and Z for any instant of time. Thus, we must solve the equations numerically, which, in practice, means that a computer does the numerical integration for us. Here, we will describe just a few results of such an integration. The analytic underpinnings for these results will be discussed later.